INTERNATIONAL JOURNAL OF
NUMERICAL ANALYSIS AND MODELING
Volume 21, Number 6, Pages 879–909

doi: 10.4208/ijnam2024-1035

VARIABLE TIME STEP METHOD OF DAHLQUIST, LINIGER AND NEVANLINNA (DLN) FOR A CORRECTED SMAGORINSKY MODEL

FARJANA SIDDIQUA AND WENLONG PEI*

Abstract. Turbulent flows strain resources, both memory and CPU speed. A family of second-order, G-stable time-stepping methods proposed by Dahlquist, Liniger, and Nevanlinna (the DLN method) has great accuracy and allows large time steps, requiring less memory and fewer FLOPS. The DLN method can also be implemented adaptively. The classical Smagorinsky model, as an effective way to approximate a resolved mean velocity, has recently been corrected to represent a flow of energy from unresolved fluctuations to the resolved mean velocity. In this paper, we apply the DLN method to one corrected Smagorinsky model and provide a detailed numerical analysis of the stability and consistency. We prove that the numerical solutions under arbitrary time step sequences are unconditionally stable in the long term and converge in second order. We also provide error estimates under certain time-step conditions. Numerical tests are given to confirm the rate of convergence and also to show that the adaptive DLN algorithm helps to control numerical dissipation so that a flow of energy from unresolved fluctuations to the resolved mean velocity is visible.

Key words. Eddy viscosity, corrected Smagorinsky model, complex turbulence, backscatter, the DLN method, G-stability, variable time-stepping.

1. Introduction

Herein we give an analysis of the method of Dahlquist, Liniger, and Nevanlinna [19] (the DLN method) for the corrected Smagorinsky model (CSM henceforth) [59] with variable time steps. Time adaptivity (adjusting time steps based on certain criteria) is an effective way to balance accuracy and time efficiency.

Eddy viscosity (EV) models are the most common approaches to depict the average turbulent flow of Navier-Stokes equations (NSE). Various eddy viscosity models in practical settings are proposed for analytical and numerical study [4,21,22,28,29]. In large eddy simulation (LES), backscatter is the study and measurement of the energy transfer process from small, unresolved turbulent scales to large, resolved scales in a computational fluid dynamics (CFD) simulation. Unfortunately, most EV models have difficulties in simulating backscatter or complex turbulent flow not at statistical equilibrium due to the neglect of the intermittent energy flow from fluctuations back to means. To overcome this defect, Jiang and Layton [33] derive a new eddy viscosity model from an equation describing the evolution of variance in a turbulent flow. Rong, Layton, and Zhao [57] extended the usual Baldwin-Lomax model so that the new model can account for statistical backscatter[1] without artificial negative viscosities. Recently, Siddiqua and Xie [59] have corrected the classical Smagorinsky model [60] with no new fitting parameters to reflect a flow of energy from unresolved fluctuations to means in the CSM. Most recently, Dai, Liu, Liu, Jiang, and Chen [18] proposed a new dynamic Smagorinsky model by an artificial

Received by the editors on February 23, 2024 and, accepted on July 22, 2024.
2000 *Mathematics Subject Classification.* 65M12, 65M22, 65M60, 76M10.
*Corresponding author.
[1]We will refer to the movement of energy from fluctuations back to means statistical backscatter when using ensemble averaging.

neural network for the prediction of outdoor airflow and pollutant dispersion. In the report, we give a detailed numerical analysis of the CSM [59] under arbitrary non-uniform time grids. Given bounded flow domain $\Omega \subset \mathbb{R}^d$ $(d = 2, 3)$, time interval $[0, T]$, and the prescribed body force $f(x, t)$, the pair $(w(x, t), q(x, t))$ approximate an ensemble average pair of velocity and pressure of Navier-Stokes solutions $(\overline{u}, \overline{p})$ and is governed by the following system

(1)
$$\begin{cases} w_t - \frac{C_s^4\delta^2}{\mu^2}\Delta w_t + w\cdot\nabla w - \nu\Delta w - \nabla\cdot\big((C_s\delta)^2|\nabla w|\nabla w\big) = f, & (x,t)\in\Omega\times(0,T] \\ \nabla\cdot w = 0, & (x,t)\in\Omega\times(0,T] \\ w(x,0) = w_0(x), & x\in\Omega \\ w(x,t) = 0, & (x,t)\in\partial\Omega\times(0,T] \\ \int_\Omega p(x,t)dx = 0, & t\in(0,T] \end{cases}.$$

This is an eddy viscosity model. Constant $C_s \approx 0.1$ is suggested by Lilly [42]. δ is a length scale (or grid-scale) and μ is a constant from Kolmogorov-Prandtl relation [38, 54]. ν is the kinematic viscosity and $\nu_T = (C_s\delta)^2|\nabla w|$ is the turbulent viscosity. $|\cdot|$ is the Euclidian norm on $\mathbb{R}^d$. The viscous term $\nabla\cdot\big((C_s\delta)^2|\nabla w|\nabla w\big)$ in (1) comes from the classic Smagorinsky model and the kinetic energy penalization $-\frac{C_s^4\delta^2}{\mu^2}\Delta w_t$ in (1) is newly added for the CSM. All other terms in (1) are from standard Navier-Stokes equations (NSE). In [59], the CSM model derivation and some basic properties of the CSM are developed, and two algorithms for its numerical simulation are proposed. However, the significant backscatter of model dissipation is not observed in specific examples except for Linearized Crank-Nicolson time discretization [59, page 21-22]. Besides that, constant time discretization in their algorithms (Linearized Crank-Nicolson time-stepping scheme) excludes the use of time adaptivity since the solution pattern (in terms of stability and convergence) under extreme time step ratios is hard to expect[1]. Dahlquist, Liniger, and Nevanlinna designed a one-parameter family of one-leg, second-order methods for evolutionary equations [19]. This family of one-leg methods (For convenience, we call this family the DLN method.) is proved to be G-stable (non-linear stable) under any arbitrary time grids [14–16] and hence ideal choice for time discretization of fluid models[2]. Herein we apply the fully discrete DLN algorithm (finite element space discretization) for the CSM in (1) and present a complete numerical analysis of the algorithm in Section 4. We prove that the numerical solutions on arbitrary time grids are unconditionally long-term stable, and converge to exact solutions at second order with moderate time step restrictions. Let $\{t_n\}_{n=0}^N$ be the time grids on interval $[0, T]$ and $k_n = t_{n+1} - t_n$ the local time step. w_n^h and q_n^h are numerical approximations of velocity and pressure at time t_n of the CSM in (1) respectively on certain finite element space with the diameter h. The fully discrete DLN algorithm

[1]In [19], the linearized Crank-Nicolson scheme and applying to the problem $y'(t) = \lambda(t)y(t)$ with $\mathrm{Re}(\lambda(t)) < 0$ and $\lambda(t_{2n}) = 0$. Under certain time step sequence ($k_n = 7$ and $k_{2n+1} = 1/2$), the sequence of numerical solutions satisfy $y_{2n} = (-2)^n y_0$, which implies the scheme is not stable.

[2]To the best of our knowledge, the DLN method is the *only* variable multi-step method which is both non-linearly stable and second-order accurate.

(with parameter $\theta \in [0,1]$) for the CSM in (1) at time t_{n+1} is written as follows:

$$
(2)\quad \begin{cases} \dfrac{\alpha_2 w_{n+1}^h + \alpha_1 w_n^h + \alpha_0 w_{n-1}^h}{\alpha_2 k_n - \alpha_0 k_{n-1}} - \dfrac{C_s^4 \delta^2}{\mu^2} \Delta\Big(\dfrac{\alpha_2 w_{n+1}^h + \alpha_1 w_n^h + \alpha_0 w_{n-1}^h}{\alpha_2 k_n - \alpha_0 k_{n-1}} \Big) \\ +\big(\sum_{\ell=0}^{2} \beta_\ell^{(n)} w_{n-\ell}^h \big) \cdot \nabla \big(\sum_{\ell=0}^{2} \beta_\ell^{(n)} w_{n-\ell}^h \big) - \nu \Delta \big(\sum_{\ell=0}^{2} \beta_\ell^{(n)} w_{n-\ell}^h \big) + \nabla \big(\sum_{\ell=0}^{2} \beta_\ell^{(n)} q_{n-\ell}^h \big) \\ +\nabla \cdot \Big((C_s \delta)^2 \big| \nabla \big(\sum_{\ell=0}^{2} \beta_\ell^{(n)} w_{n-\ell}^h \big) \big| \nabla \big(\sum_{\ell=0}^{2} \beta_\ell^{(n)} w_{n-\ell}^h \big) \Big) = f\big(\sum_{\ell=0}^{2} \beta_\ell^{(n)} t_{n-\ell} \big), \\ \nabla \cdot w_{n+1}^h = 0, \end{cases}
$$

for $1 \le n \le N-1$. Here the coefficients in (2) are

$$
\begin{bmatrix} \alpha_2 \\ \alpha_1 \\ \alpha_0 \end{bmatrix} = \begin{bmatrix} \frac{1}{2}(\theta+1) \\ -\theta \\ \frac{1}{2}(\theta-1) \end{bmatrix}, \quad \begin{bmatrix} \beta_2^{(n)} \\ \beta_1^{(n)} \\ \beta_0^{(n)} \end{bmatrix} = \begin{bmatrix} \frac{1}{4}\Big(1 + \frac{1-\theta^2}{(1+\varepsilon_n\theta)^2} + \varepsilon_n^2 \frac{\theta(1-\theta^2)}{(1+\varepsilon_n\theta)^2} + \theta\Big) \\ \frac{1}{2}\Big(1 - \frac{1-\theta^2}{(1+\varepsilon_n\theta)^2}\Big) \\ \frac{1}{4}\Big(1 + \frac{1-\theta^2}{(1+\varepsilon_n\theta)^2} - \varepsilon_n^2 \frac{\theta(1-\theta^2)}{(1+\varepsilon_n\theta)^2} - \theta\Big) \end{bmatrix}.
$$

The step variability $\varepsilon_n = (k_n - k_{n-1})/(k_n + k_{n-1}) \in (-1,1)$ is the function of two step sizes and $\varepsilon_n \in (-1,1)$.

The main result of this article is the complete numerical analysis of the DLN method in Section 4 and computational tests in Section 5 showing backscatter phenomena for the CSM model (1). The paper is organized as follows. We provide necessary notations and preliminaries for numerical analysis in Section 2, and present the fully discrete variational formulation in Section 3. We show that the DLN solutions are long-term, unconditional stable in Theorem 4.5 of Section 4.1 and perform the variable step error analysis with the moderate time step restriction in Theorem 4.8 of Section 4.2. Furthermore, we present the test problem with exact solutions [23] in Section 5.1, to confirm the fully discrete DLN algorithm is second-order in time, and a test problem about the flow between offset cylinders [32] in Section 5.2 to check the unconditional stability and the efficiency of the time adaptivity of the DLN algorithm.

1.1. Related Work. Smagorinsky model and other large eddy viscosity models have been studied and corrected in numerous works [1, 3, 12, 37, 39, 49, 50]. Meanwhile, various efficient numerical schemes have been designed to address the complexity of the Smagorinsky model and other turbulence models [20, 34, 51, 52, 58]. Due to the fine properties of stability and consistency, the whole DLN family calls great attention to the simulation of evolutionary equations and fluid models. The DLN method with $\theta = \frac{2}{3}$ is suggested in [19] to relieve the conflict between error and stability. Kulikov and Shindin find that the DLN method with $\theta = \frac{2}{\sqrt{5}}$ has the best stability at infinity [40]. The midpoint rule (the DLN method with $\theta = 1$), conserving all quadratic Hamiltonians, has been thoroughly studied and widely used in computational fluid dynamics [2, 5, 7–9, 26, 43]. Recently, the whole DLN family has been applied to some time-dependent fluid models and shows its outstanding performance in some specific examples [46, 53, 55, 56]. In addition, the DLN implementation has been simplified by the re-factorization process (adding time filters on backward Euler method) for wide application [47]. Time adaptivity of the DLN method (by the local truncation error criterion) is proposed to solve stiff differential systems for both efficiency and accuracy [48].

2. Notations and preliminary results

In this section, we introduce necessary notations and preliminary results. Recall that $\Omega \subset \mathbb{R}^d$ $(d = 2,\ 3)$ is the bounded domain of the CSM in eq. (1). Banach space $L^p(\Omega)$ $(p \geq 1)$ contains all Lebesgue measurable function f such that $|f|^p$ is integrable. For $r \in \{0\} \cup \mathbb{N}$, Sobolev space $W^{m,p}(\Omega)$ with norm $\|.\|_{m,p}$ contains all functions whose weak derivatives up to m-th belong to $L^p(\Omega)$. Thus $W^{m,p}(\Omega)$ is exactly L^p when $m = 0$. We use H^m with norm $\|\cdot\|_m$ and semi-norm $|\cdot|_m$ to denote the inner product space $W^{m,2}(\Omega)$. $\|\cdot\|$ and $(\cdot,\cdot)$ denote the $L^2(\Omega)$ norm and inner product, respectively. The solution spaces X for the velocity and Q for the pressure are defined as:

$$X = \Big\{v \in \big(L^3(\Omega)\big)^d : \nabla v \in \big(L^3(\Omega)\big)^{d\times d},\ v\big|_{\partial\Omega} = 0\Big\},\ Q = \Big\{q \in L^2(\Omega) : \int_\Omega q\ dx = 0\Big\},$$

and the divergence-free velocity space is

$$V = \big\{v \in X : (q, \nabla\cdot v) = 0,\ \forall q \in Q\big\}.$$

X' is the dual norm of X with the dual norm

$$\|f\|_{-1} = \sup_{0\neq v\in X} \frac{(f,v)}{\|\nabla v\|}, \qquad \forall f \in X'.$$

Definition 2.1. *(Trilinear Form) Define the trilinear form $b^* : X \times X \times X \to \mathbb{R}$ as follows*

$$b^*(u,v,w) := \frac{1}{2}(u\cdot\nabla v, w) - \frac{1}{2}(u\cdot\nabla w, v), \qquad \forall u, v, w \in X.$$

Lemma 2.2. *The nonlinear term $b^*(\cdot,\cdot,\cdot)$ is continuous on $X \times X \times X$ (and thus on $V \times V \times V$) which has the following skew-symmetry property,*

$$b^*(u,v,w) = -b^*(u,w,v), \qquad b^*(u,v,v) = 0. \tag{3}$$

As a consequence, we get

$$b^*(u,v,w) = (u\cdot\nabla v, w), \quad \forall\ u \in V \text{and } v,\ w \in X,$$
$$b^*(u,v,v) = 0, \quad \forall\ u,\ v \in X.$$

Proof. Proof of this lemma is standard, see $p.114$ of Girault and Raviart [24]. □

Lemma 2.3. *For any $u,\ v,\ w \in X$*

$$\begin{aligned} b^*(u,v,w) &\leq C(\Omega)\|\nabla u\|\|\nabla v\|\|\nabla w\|, \\ b^*(u,v,w) &\leq C(\Omega)\|u\|^{1/2}\|\nabla u\|^{1/2}\|\nabla v\|\|\nabla w\|. \end{aligned} \tag{4}$$

Proof. By Hölder's inequality, Poincaré-Friedrichs's inequality and Ladyzhenskaya's inequality. □

Next is a Discrete Grönwall Lemma, see [27, Lemma 5.1, p.369].

Lemma 2.4. *Let Δt, B be non-negative real numbers and $\{a_n\}_{n=0}^\infty$, $\{b_n\}_{n=0}^\infty$, $\{c_n\}_{n=0}^\infty$, $\{d_n\}_{n=0}^\infty$ be non-negative sequences of real numbers such that*

$$a_\ell + \Delta t\sum_{n=0}^{\ell} b_n \leq \Delta t\sum_{n=0}^{\ell} d_n a_n + \Delta t\sum_{n=0}^{\ell} c_n + B, \qquad \forall \ell \in \mathbb{N},$$

and $\Delta t d_n < 1$ for all n, then

$$a_\ell + \Delta t\sum_{n=0}^{\ell} b_n \leq \exp\Big(\Delta t\sum_{n=0}^{\ell}\frac{d_n}{1-\Delta t d_n}\Big)\Big(\Delta t\sum_{n=0}^{\ell} c_n + B\Big), \qquad \forall \ell \in \mathbb{N}.$$

Proof. See [27, p.369]. □

Lemma 2.5. *(***Strong Monotonicity (SM) and Local Lipschitz Continuity (LLC)***) For any* $u,\ v,\ w \in W^{1,3}(\Omega)$

(**SM**) $$(|\nabla u|\nabla u - |\nabla w|\nabla w, \nabla(u-w)) \geq C_1 \|\nabla(u-w)\|_{0,3}^3,$$

(**LLC**)
$$(|\nabla u|\nabla u - |\nabla w|\nabla w, \nabla v) \leq C_2 \big(\max\{\|\nabla u\|_{0,3}, \|\nabla w\|_{0,3}\}\big) \|\nabla(u-w)\|_{0,3} \|\nabla v\|_{0,3},$$

where $C_1,\ C_2$ are positive constants independent of u, v, w.

Proof. We refer to [17, 36, 44] for proof. □

Let $\mathcal{T}_h$ be the edge-to-edge triangulation of the domain Ω with diameter $h > 0$. $X^h \subset X$ and $Q^h \subset Q$ are certain finite element spaces of velocity and pressure respectively. The divergence-free subspace of X^h is

$$V^h := \Big\{ v^h \in X^h : (p^h, \nabla \cdot v^h) = 0, \quad \forall p^h \in Q^h \Big\}.$$

Given $(w, q) \in X \times Q$, we assume that the corresponding finite element pair (X^h, Q^h) satisfies

$$\begin{aligned} &X^h : C^m\text{-space containing polynomials of highest degree } r \ (r \in \mathbb{N}), \\ &Q^h : C^m\text{-space containing polynomials of highest degree } s \ (s \in \mathbb{N}). \end{aligned} \tag{5}$$

We have the following approximations (See [6, 13] for proof):

$$\begin{aligned} &\inf_{v^h \in X^h} \|w - v^h\|_{\ell_1} \leq C h^{r+1-\ell_1} |w|_{r+1}, \quad w \in (H^{r+1})^d \cap X, \\ &\inf_{p^h \in Q^h} \|q - p^h\|_{\ell_2} \leq C h^{s+1-\ell_2} |q|_{s+1}, \quad q \in H^{s+1} \cap Q. \end{aligned} \tag{6}$$

where $0 \leq \ell_1 \leq \min\{m+1, r+1\}$ and $0 \leq \ell_2 \leq \min\{m+1, s+1\}$. We need the $L^p - L^2$-type inverse inequality [44].

Theorem 2.6. *Let* Θ *be the minimum angle in the triangulation of domain* $\Omega \subset \mathbb{R}^d$ *(*$d = 2, 3$*) and* X^h *be the finite element space with highest polynomial degree* r*. For any* $v^h \in X^h$ *and* $2 \leq p < \infty$*, there is a constant* $C = C(\Theta, p, r) > 0$ *such that*

$$\|\nabla^h v^h\|_{0,p} \leq C h^{\frac{d}{2}(\frac{2-p}{p})} \|\nabla^h v^h\|, \tag{7}$$

where ∇^h *is the element-wise defined gradient operator.*

Proof. See [44, p.349-350] for proof. □

We assume that (X^h, Q^h) satisfies the discrete inf-sup condition:

$$\inf_{p^h \in Q^h} \sup_{v^h \in X^h} \frac{(p^h, \nabla \cdot v^h)}{\|p^h\| \|\nabla v^h\|} \geq C_{\text{is}}^h, \tag{8}$$

where C_{is}^h is a positive constant independent of h. We define the Stokes projection $\big(I_{\text{St}}^h w, I_{\text{St}}^h q\big) \in V^h \times Q^h$ to be the solution of the following problem

$$\begin{aligned} \nu(\nabla w, \nabla v^h) - (q, \nabla \cdot v^h) &= \nu(\nabla I_{\text{St}}^h w, \nabla v^h) - (I_{\text{St}}^h q, \nabla \cdot v^h), \quad \forall v^h \in X^h \\ -(p^h, \nabla \cdot I_{\text{St}}^h w) &= 0, \qquad\qquad\qquad\qquad\qquad\qquad\quad \forall p^h \in Q^h. \end{aligned} \tag{9}$$

We need the following the approximation properties of the Stokes projection if the finite element spaces X^h and Q^h satisfy the discrete inf-sup condition in (8) (see [25, 35] for proof)

$$
\begin{aligned}
|w - I^h_{\mathrm{St}} w|_1 \leq & 2\Big(1 + \frac{1}{C^h_{\mathrm{is}}}\Big) \inf_{v^h \in X^h} |w - v^h|_1 + \nu^{-1} \inf_{p^h \in Q^h} \|q - p^h\|, \\
\|w - I^h_{\mathrm{St}} w\| \leq & \Big(\nu^{-1} \inf_{p^h \in Q^h} \|q - p^h\| + \inf_{v^h \in X^h} |w - v^h|_1\Big) \\
& \times \sup_{\hat{g} \in L^2(\Omega)\setminus\{0\}} \frac{1}{\|\hat{g}\|}\Big(\nu^{-1} \inf_{q^h \in Q^h} \|\xi_{\hat{g}} - p^h\| + \inf_{v^h \in V^h} |\phi_{\hat{g}} - v^h|_1\Big),
\end{aligned} \tag{10}
$$

where the pair $(\phi_{\hat{g}}, \xi_{\hat{g}}) \in X \times Q$ is the solution to the dual Stokes problem

$$
\begin{aligned}
\nu(\nabla v, \nabla \phi_{\hat{g}}) + (\nabla \cdot v, \xi_{\hat{g}}) &= (\hat{g}, v), \quad \forall v \in X, \\
(\nabla \cdot \phi_{\hat{g}}, p) &= 0, \qquad \forall p \in Q.
\end{aligned}
$$

3. The variable step DLN method for CSM

We denote $w(t_n)$ by w_n and $q(t_n)$ by q_n in the CSM in (1). $w^h_n \in X^h$ and $q^h_n \in Q^h$ represent the DLN solutions of w_n and q_n respectively. For convenience, we denote

$$
\begin{aligned}
t_{n,\beta} &= \sum_{\ell=0}^{2} \beta^{(n)}_\ell t_{n-1+\ell}, \qquad w_{n,\beta} = \sum_{\ell=0}^{2} \beta^{(n)}_\ell w(t_{n-1+\ell}), \qquad w^h_{n,\beta} = \sum_{\ell=0}^{2} \beta^{(n)}_\ell w^h_{n-1+\ell}, \\
q_{n,\beta} &= \sum_{\ell=0}^{2} \beta^{(n)}_\ell q(t_{n-1+\ell}), \qquad q^h_{n,\beta} = \sum_{\ell=0}^{2} \beta^{(n)}_\ell q^h_{n-1+\ell}, \qquad f_{n,\beta} = \sum_{\ell=0}^{2} \beta^{(n)}_\ell f(t_{n-1+\ell}),
\end{aligned}
$$

and represent the average time step $\alpha_2 k_n - \alpha_0 k_{n-1}$ by $\widehat{k}_n$. The variational formulation of the variable time-stepping DLN scheme (with grad-div stabilizer [11]) in (2) is: given $w^h_n,\ w^h_{n-1} \in X^h$ and $q^h_n,\ q^h_{n-1} \in Q^h$, find w^h_{n+1} and q^h_{n+1} satisfying

$$
\begin{aligned}
&\Big(\frac{\alpha_2 w^h_{n+1} + \alpha_1 w^h_n + \alpha_0 w^h_{n-1}}{\widehat{k_n}}, v^h\Big) + \frac{C_s^4 \delta^2}{\mu^2}\Big(\frac{\alpha_2 \nabla w^h_{n+1} + \alpha_1 \nabla w^h_n + \alpha_0 \nabla w^h_{n-1}}{\widehat{k_n}}, \nabla v^h\Big) \\
&+ \nu(\nabla w^h_{n,\beta}, \nabla v^h) + b^*(w^h_{n,\beta}, w^h_{n,\beta}, v^h) + \gamma(\nabla \cdot w^h_{n,\beta}, \nabla \cdot v^h) - (q^h_{n,\beta}, \nabla \cdot v^h) \\
&+ \Big((C_s\delta)^2 |\nabla w^h_{n,\beta}| \nabla w^h_{n,\beta}, \nabla v^h\Big) = (f_{n,\beta}, v^h), \qquad \forall v^h \in X^h, \\
&(\nabla \cdot w^h_{n,\beta}, p^h) = 0, \qquad \forall p^h \in Q^h,
\end{aligned} \tag{11}
$$

where constant $\gamma > 0$ needs to be decided by specific problems. Let $\widetilde{w^h_n}$ denote the standard (second order) linear extrapolation [45] of w^h_n

$$
\widetilde{w^h_n} = \beta^{(n)}_2 \left\{ \left(1 + \frac{k_n}{k_{n-1}}\right) w^h_n - \left(\frac{k_n}{k_{n-1}}\right) w^h_{n-1} \right\} + \beta^{(n)}_1 w^h_n + \beta^{(n)}_0 w^h_{n-1}.
$$

After applying the linearly implicit DLN scheme for time discretization, we get the following discretization:

$$
\begin{aligned}
&\Big(\frac{\alpha_2 w^h_{n+1}+\alpha_1 w^h_n+\alpha_0 w^h_{n-1}}{\widehat{k_n}},v^h\Big)+\frac{C_s^4\delta^2}{\mu^2}\Big(\frac{\alpha_2\nabla w^h_{n+1}+\alpha_1\nabla w^h_n+\alpha_0\nabla w^h_{n-1}}{\widehat{k_n}},\nabla v^h\Big)\\
&+\nu(\nabla w^h_{n,\beta},\nabla v^h)+b^*(\widetilde{w^h_n},w^h_{n,\beta},v^h)+\gamma(\nabla\cdot w^h_{n,\beta},\nabla\cdot v^h)\\
&-(q^h_{n,\beta},\nabla\cdot v^h)+\Big((C_s\delta)^2|\nabla\widetilde{w^h_n}|\nabla w^h_{n,\beta},\nabla v^h\Big)=(f(t_{n,\beta}),v^h),\ \forall v^h\in X^h,\\
&(\nabla\cdot w^h_{n,\beta},p^h)=0,\ \forall p^h\in Q^h.
\end{aligned}
\tag{12}
$$

4. Numerical Analysis

We define the discrete Bochner space with time grids $\{t_n\}_{n=0}^N$ on time interval $[0,T]$,

$$
\begin{aligned}
\ell^\infty\big(0,N;(W^{m,p})^d\big)&:=\big\{f(\cdot,t)\in(W^{m,p})^d:|||f|||_{\infty,m,p}<\infty\big\},\\
\ell^{p_1,\beta}\big(0,N;(W^{m,p_2})^d\big)&:=\big\{f(\cdot,t)\in(W^{m,p_2})^d:|||f|||_{p_1,m,p_2,\beta}<\infty\big\},
\end{aligned}
$$

where the corresponding discrete norms are

$$
|||f|||_{\infty,m,p}:=\max_{0\le n\le N}\|f(\cdot,t_n)\|_{m,p},\ |||f|||_{p_1,m,p_2,\beta}:=\Big(\sum_{n=1}^N(k_n+k_{n-1})\|f(\cdot,t_{n,\beta})\|^{p_1}_{m,p_2}\Big)^{\frac{1}{p_1}}.
$$

Definition 4.1. *For $0\le\theta\le 1$, define the semi-positive symmetric definite matrix $G(\theta)$ by*

$$
G(\theta)=\begin{bmatrix}\frac{1}{4}(1+\theta)\mathbb{I}_d & 0\\ 0 & \frac{1}{4}(1-\theta)\mathbb{I}_d\end{bmatrix}.
$$

We present two Lemmas about the stability and consistency of the DLN method.

Lemma 4.2. *Let $\{y_n\}_{n=0}^N$ be any sequence in $\big(L^2(\Omega)\big)^d$. For any $\theta\in[0,1]$ and $n\in\{1,2,\cdots,N-1\}$, we have*

$$
\Big(\sum_{\ell=0}^2\alpha_\ell y_{n-1+\ell},\sum_{\ell=0}^2\beta^{(n)}_\ell y_{n-1+\ell}\Big)=\left\|\begin{matrix}y_{n+1}\\ y_n\end{matrix}\right\|^2_{G(\theta)}-\left\|\begin{matrix}y_n\\ y_{n-1}\end{matrix}\right\|^2_{G(\theta)}+\Big\|\sum_{\ell=0}^2\lambda^{(n)}_\ell y_{n-1+\ell}\Big\|^2,
\tag{13}
$$

where the $\|\cdot\|_{G(\theta)}$-norm is

$$
\left\|\begin{matrix}u\\ v\end{matrix}\right\|^2_{G(\theta)}=[u^{\rm tr},v^{\rm tr}]G(\theta)\begin{bmatrix}u\\ v\end{bmatrix}=\frac{1}{4}(1+\theta)\|u\|^2+\frac{1}{4}(1-\theta)\|v\|^2,\quad\forall u,v\in\big(L^2(\Omega)\big)^d,
\tag{14}
$$

where tr *means transpose of any vector and the coefficients $\{\lambda^{(n)}_\ell\}_{\ell=0}^2$ are*

$$
\lambda^{(n)}_1=-\frac{\theta(1-\theta^2)}{\sqrt{2}(1+\varepsilon_n\theta)},\qquad\lambda^{(n)}_2=-\frac{1-\varepsilon_n}{2}\lambda^{(n)}_1,\qquad\lambda^{(n)}_0=-\frac{1+\varepsilon_n}{2}\lambda^{(n)}_1.
\tag{15}
$$

Proof. The proof of identity in (13) is just algebraic calculation. □

Remark 4.3. *If we replace $\big(L^2(\Omega)\big)^d$ by Euclidian space $\mathbb{R}$, the identity in* (13) *still holds and implies G-stability of the DLN method with $\theta\in[0,1)$. Recall the definition of G-stability for the one-leg, m-step scheme with constant step k [15]:*

$$
\sum_{\ell=0}^m\alpha_\ell y_{n+1-\ell}=kf\big(\sum_{\ell=0}^m\beta_\ell t_{n+1-\ell},\sum_{\ell=0}^m\beta_\ell y_{n+1-\ell}\big).
$$

The above scheme satisfies G-stability condition if there exists a real symmetric positive definite matrix $G = [g_{ij}]_{i,j=1}^{m}$ *such that for all* n

$$Y_{n+1}^{tr} G Y_{n+1} - Y_n^{tr} G Y_n \leq 2k\Big(f\big(\sum_{\ell=0}^{m} \beta_\ell t_{n+1-\ell}, \sum_{\ell=0}^{m} \beta_\ell y_{n+1-\ell}\big), \sum_{\ell=0}^{m} \beta_\ell y_{n+1-\ell}\Big).$$

where $Y_n = [y_n, y_{n-1}, \cdots, y_{n-m+1}]^{\mathrm{tr}}$. *The above G-stability inequality ensures that the deviation from the initial condition in (in G-norm) controls the deviations from the sequence of solutions at later times based on that initial condition. From the G-stability identity in* (13), *the DLN method with* $\theta \in [0, 1)$ *is G-stable. For the case* $\theta = 1$, *the DLN method with* $\theta = 1$ *is reduced to the one-step midpoint rule and its G-stability property is easy to check by definition.*

Lemma 4.4. *Let* Y *be any Banach space over* $\mathbb{R}$ *with norm* $\|\cdot\|_Y$, $\{t_n\}_{n=0}^{N}$ *be time grids on time interval* $[0, T]$ *and* u *be the mapping from* $[0, T]$ *to* Y. *We set*

$$k_{\max} = \max_{0 \leq n \leq N-1} \{k_n\},$$

and assume that the mapping $u(t)$ *is smooth enough about the variable* t, *then for any* $\theta \in [0, 1]$,

$$\Big\| \sum_{\ell=0}^{2} \beta_\ell^{(n)} u(t_{n-1+\ell}) - u(t_{n,\beta}) \Big\|_Y^2 \leq C(\theta) k_{\max}^3 \int_{t_{n-1}}^{t_{n+1}} \|u_{tt}\|_Y^2 dt,$$

$$\Big\| \frac{1}{\widehat{k}_n} \sum_{\ell=0}^{2} \alpha_\ell u(t_{n-1+\ell}) - u_t(t_{n,\beta}) \Big\|_Y^2 \leq C(\theta) k_{\max}^3 \int_{t_{n-1}}^{t_{n+1}} \|u_{ttt}\|_Y^2 dt. \tag{16}$$

Proof. We use Taylor's Theorem and expand $u(t_{n+1})$, $u(t_n)$, $u(t_{n-1})$ at $t_{n,\beta}$. By Hölder's inequality, we obtain (16). □

4.1. Stability of the DLN scheme for the CSM. The DLN method is a one parameter family of A-stable, 2 step, G-stable methods ($0 \leq \theta \leq 1$). It reduces to the one-step midpoint scheme if $\theta = 1$. Moreover, the $G(\theta)$-norm in (14) does not depend on the time step ratio. In this Subsection, we prove the unconditional, long-time, variable time step energy-stability of (11) by using the G-stability property (lemma 4.2) of the method.

Theorem 4.5. *The one-leg variable time step DLN scheme by* (11) *is unconditionally, long-time stable, i.e. for any integer* $N > 1$,

$$\begin{aligned}
&\frac{1+\theta}{4}\big(\|w_N^h\|^2 + \frac{C_s^4\delta^2}{\mu^2}\|\nabla w_N^h\|^2\big) + \frac{1-\theta}{4}\big(\|w_{N-1}^h\|^2 + \frac{C_s^4\delta^2}{\mu^2}\|\nabla w_{N-1}^h\|^2\big) \\
&+\sum_{n=1}^{N-1}\Big(\Big\|\sum_{\ell=0}^{2}\lambda_\ell^{(n)} w_{n-1+\ell}^h\Big\|^2 + \frac{C_s^4\delta^2}{\mu^2}\Big\|\sum_{\ell=0}^{2}\lambda_\ell^{(n)}\nabla w_{n-1+\ell}^h\Big\|^2\Big) + \sum_{n=1}^{N-1}\widehat{k}_n\big(\frac{\nu}{2}\|\nabla w_{n,\beta}^h\|^2 + \gamma\|\nabla\cdot w_{n,\beta}^h\|^2\big) \\
&+\sum_{n=1}^{N-1}\widehat{k}_n\int_\Omega\big[(C_s\delta)^2|\nabla w_{n,\beta}^h|\big]|\nabla w_{n,\beta}^h|^2 dx \leq \frac{C(\theta)k_{\max}^4}{\nu}\|f_{tt}\|_{L^2(0,T;X')}^2 + \frac{1}{\nu}|||f|||_{2,-1,2,\beta}^2 \\
&\quad+\frac{1+\theta}{4}\big(\|w_1^h\|^2 + \frac{C_s^4\delta^2}{\mu^2}\|\nabla w_1^h\|^2\big) + \frac{1-\theta}{4}\big(\|w_0^h\|^2 + \frac{C_s^4\delta^2}{\mu^2}\|\nabla w_0^h\|^2\big).
\end{aligned} \tag{17}$$

Proof. We set $v^h = w^h_{n,\beta}$, $p^h = q^h_{n,\beta}$ in (11). By lemma 2.2 and identity (13) in lemma 4.2, we obtain

$$\Big(\sum_{\ell=0}^{2}\alpha_\ell w^h_{n-1+\ell}, w^h_{n,\beta}\Big) + \frac{C_s^4\delta^2}{\mu^2}\Big(\sum_{\ell=0}^{2}\alpha_\ell \nabla w^h_{n-1+\ell}, \nabla w^h_{n,\beta}\Big) + \gamma\widehat{k}_n\|\nabla\cdot w^h_{n,\beta}\|^2$$
$$+\widehat{k}_n\int_\Omega \big(\nu + (C_s\delta)^2|\nabla w^h_{n,\beta}|\big)|\nabla w^h_{n,\beta}|^2\,dx = \widehat{k}_n(f_{n,\beta}, w^h_{n,\beta})$$
$$\le \widehat{k}_n\|f_{n,\beta}\|_{-1}\|\nabla w^h_{n,\beta}\|.$$

The G-stability identity (13) in Lemma 4.2 implies

(18)
$$\left\|\begin{matrix} w^h_{n+1}\\ w^h_n\end{matrix}\right\|^2_{G(\theta)} - \left\|\begin{matrix} w^h_n\\ w^h_{n-1}\end{matrix}\right\|^2_{G(\theta)} + \Big\|\sum_{\ell=0}^{2}\lambda^{(n)}_\ell w^h_{n-1+\ell}\Big\|^2 + \widehat{k}_n\int_\Omega\Big(\frac{\nu}{2} + (C_s\delta)^2|\nabla w^h_{n,\beta}|\Big)|\nabla w^h_{n,\beta}|^2 dx$$
$$+\gamma\widehat{k}_n\|\nabla\cdot w^h_{n,\beta}\|^2 + \frac{C_s^4\delta^2}{\mu^2}\Big(\left\|\begin{matrix}\nabla w^h_{n+1}\\ \nabla w^h_n\end{matrix}\right\|^2_{G(\theta)} - \left\|\begin{matrix}\nabla w^h_n\\ \nabla w^h_{n-1}\end{matrix}\right\|^2_{G(\theta)} + \Big\|\sum_{\ell=0}^{2}\lambda^{(n)}_\ell \nabla w^h_{n-1+\ell}\Big\|^2\Big)$$
$$\le \frac{\widehat{k}_n}{2\nu}\|f_{n,\beta}\|^2_{-1}.$$

By triangle inequality and (16) in lemma 4.4, we get

$$\frac{\widehat{k}_n}{2\nu}\|f_{n,\beta}\|^2_{-1} \le \frac{\widehat{k}_n}{\nu}\|f_{n,\beta} - f(t_{n,\beta})\|^2_{-1} + \frac{\widehat{k}_n}{\nu}\|f(t_{n,\beta})\|^2_{-1}$$
$$\le \frac{C(\theta)k^4_{\max}}{\nu}\int_{t_{n-1}}^{t_{n+1}}\|f_{tt}\|^2_{-1}dt + \frac{(k_n + k_{n-1})}{\nu}\|f(t_{n,\beta})\|^2_{-1}.$$

We sum (18) over n from 1 to $N-1$ and have the desired result in (17). □

Remark 4.6. *We identify the following quantities from the energy equality in* (17)*:*

(1) Model kinetic energy,

$$\mathcal{E}^{\mathtt{EN}}_N = \frac{1+\theta}{4}\big(\|w^h_N\|^2 + \frac{C_s^4\delta^2}{\mu^2}\|\nabla w^h_N\|^2\big) + \frac{1-\theta}{4}\big(\|w^h_{N-1}\|^2 + \frac{C_s^4\delta^2}{\mu^2}\|\nabla w^h_{N-1}\|^2\big).$$

(2) Energy dissipation due to viscous force,

$$\mathcal{E}^{\mathtt{VD}}_N = \nu\|\nabla w^h_{N-1,\beta}\|^2.$$

(3) Eddy viscosity dissipation,

$$\mathcal{E}^{\mathtt{EVD}}_N = \int_\Omega \big[(C_s\delta)^2|\nabla w^h_{N-1,\beta}|\big]|\nabla w^h_{N-1,\beta}|^2\,dx.$$

(4) Numerical dissipation,

$$\mathcal{E}^{\mathtt{ND}}_N = \left\|\frac{\sum_{l=0}^{2}\lambda_l^{N-1}w^h_{N-2+l}}{\sqrt{\widehat{k}_{N-1}}}\right\|^2 + \frac{C_s^4\delta^2}{\mu^2}\left\|\frac{\sum_{l=0}^{2}\lambda_l^{N-1}\nabla w^h_{N-2+l}}{\sqrt{\widehat{k}_{N-1}}}\right\|^2.$$

$\mathcal{E}^{\mathtt{ND}}_N$ *vanishes if and only if* $\theta \in \{0,1\}$.

(5) The model dissipation originating from the CSM in (1)*,*

$$\mathcal{E}^{\mathtt{MD}}_N = \frac{C_s^4\delta^2}{\widehat{k}_{N-1}\mu^2}\Big(\left\|\begin{matrix}\nabla w^h_N\\ \nabla w^h_N\end{matrix}\right\|^2_{G(\theta)} - \left\|\begin{matrix}\nabla w_{N-1}\\ \nabla w_{N-1}\end{matrix}\right\|^2_{G(\theta)} + \Big\|\sum_{\ell=0}^{2}\lambda^{(N-1)}_\ell \nabla w^h_{N-2+\ell}\Big\|^2\Big)$$
$$+\int_\Omega\big[(C_s\delta)^2|\nabla w^h_{N-1,\beta}|\big]|\nabla w^h_{N-1,\beta}|^2 dx.$$

Model dissipation in this paper can be positive or negative. When it is positive, it aggregates energy from mean to fluctuations. When negative, energy is transferred from fluctuations back to the mean.

Remark 4.7. *The one-leg linearly implicit DLN method by (12) is unconditionally, long-time stable, i.e. for any integer $N > 1$,*

$$\begin{aligned}(19)\quad &\frac{1+\theta}{4}\big(\|w_N^h\|^2+\frac{C_s^4\delta^2}{\mu^2}\|\nabla w_N^h\|^2\big)+\frac{1-\theta}{4}\big(\|w_{N-1}^h\|^2+\frac{C_s^4\delta^2}{\mu^2}\|\nabla w_{N-1}^h\|^2\big)\\ &+\sum_{n=1}^{N-1}\Big(\big\|\sum_{\ell=0}^{2}\lambda_\ell^{(n)}w_{n-1+\ell}^h\big\|^2+\frac{C_s^4\delta^2}{\mu^2}\big\|\sum_{\ell=0}^{2}\lambda_\ell^{(n)}\nabla w_{n-1+\ell}^h\big\|^2\Big)+\sum_{n=1}^{N-1}\widehat{k}_n\big(\frac{\nu}{2}\|\nabla w_{n,\beta}^h\|^2+\gamma\|\nabla\cdot w_{n,\beta}^h\|^2\big)\\ &+\sum_{n=1}^{N-1}\widehat{k}_n\int_\Omega\big[(C_s\delta)^2|\widetilde{w_{n,\beta}^h}|\big]|\nabla w_{n,\beta}^h|^2dx\le\frac{C(\theta)k_{\max}^4}{\nu}\|f_{tt}\|_{L^2(0,T;X')}^2+\frac{1}{\nu}|||f|||_{2,-1,\beta}^2\\ &\quad+\frac{1+\theta}{4}\big(\|w_1^h\|^2+\frac{C_s^4\delta^2}{\mu^2}\|\nabla w_1^h\|^2\big)+\frac{1-\theta}{4}\big(\|w_0^h\|^2+\frac{C_s^4\delta^2}{\mu^2}\|\nabla w_0^h\|^2\big).\end{aligned}$$

4.2. Error Analysis of the DLN Scheme for the CSM. In this Subsection, we analyze the error between the semi-discrete solution and the fully discrete solution to (1) in Theorem 4.8 under the following time step condition[1]:

$$(20)\qquad \frac{C(\theta)}{\nu^3}\big(\widehat{k}_{n+1}\|\nabla w_{n+1,\beta}\|^4+\widehat{k}_n\|\nabla w_{n,\beta}\|^4+\widehat{k}_{n-1}\|\nabla w_{n-1,\beta}\|^4\big)<1,\qquad\forall n.$$

Theorem 4.8. *Let $(w(t),q(t))$ be sufficiently smooth, strong solutions of the CSM. We assume that the velocity $w\in X$, pressure $q\in Q$, body force f of the CSM in* (1) *satisfy*

$$\begin{aligned}&w\in\ell^{2,\beta}(0,N;(H^{r+1})^d)\cap\ell^{4,\beta}(0,N;(H^{r+1})^d)\cap\ell^{3,\beta}(0,N;(H^{r+1})^d)\cap\ell^{3,\beta}(0,N;(W^{1,3})^d),\\ &\qquad w_t\in L^2\big(0,T;(H^{r+1})^d\big),\qquad w_{ttt}\in L^2\big(0,T;(H^1)^d\big),\\ &w_{tt}\in L^2\big(0,T;(H^{r+1})^d\big)\cap L^3\big(0,T;(W^{1,3})^d\big)\cap L^3\big(0,T;(H^{r+1})^d\big)\cap L^4\big(0,T;(H^{r+1})^d\big),\\ &\qquad q\in\ell^{2,\beta}(0,N;H^{s+1}),\qquad f_{tt}\in L^2(0,T;X'),\end{aligned}$$

and the finite element spaces X^h, Q^h satisfies the discrete inf-sup condition in (8) *and approximations in* (6)*. Under the time step condition in* (20)*, the variable time-stepping DLN scheme (with $\theta\in[0,1]$) for the CSM in* (11) *satisfies: for $r,\ s,\in\{0\}\cup\mathbb{N}$ and any integer $N\ge 2$*

$$\begin{aligned}(21)\qquad &\max_{0\le n\le N}\|w_n^h-w_n\|+C(\theta)\sqrt{\nu}\Big(\sum_{n=1}^{N-1}\widehat{k}_n\|\nabla(w_{n,\beta}^h-w_{n,\beta})\|^2\Big)^{1/2}\\ &\le\mathcal{O}\big(k_{\max}^2,h^r,h^{s+1},\delta h^{\frac{3r}{4}-\frac{d}{8}},\delta k_{\max}^{3/2}\big).\end{aligned}$$

Remark 4.9. *Since δ has the same dimension as h, the spatial convergence rate in* (21) *is $\min\{r,s+1\}$ as long as the highest polynomial degree for velocity $r\in\{1,2\}$. Thus the DLN algorithm in* (2) *is second-order accurate in both time and space if we choose Taylor-Hood $\mathbb{P}2-\mathbb{P}1$ finite element space and set the time step $\Delta t\approx h$.*

Proof. The proof is relatively long, thus we devide the rest of proof into four parts:

1. We combine CSM at time $t_{n,\beta}$ and the DLN algorithm for CSM in (11) to derive the equation of pointwise error $e_{n+1}:=w_{n+1}-w_{n+1}^h$.

[1]To our best knowledge, time step conditions like $\Delta t<\mathcal{O}(\nu^{-3})$ cannot be avoided for fully-implicit schemes in error analysis.

2. We set W_n to be the velocity component of Stokes projection $(w_n, 0)$ onto $V^h \times Q^h$ and decompose the error to be $e_n = (w_n - W_n) - (w_n^h - W_n) := \eta_n - \phi_n^h$. Then we transfer the error equation to be the new equation in terms of $\{\eta_{n-1+\ell}\}_{\ell=0}^2$ and $\{\phi_{n-1+\ell}\}_{\ell=0}^2$.
3. We obtain the bound for ϕ_{n+1}^h by addressing the terms from
   - the newly added kinetic energy penalization in the CSM,
   - the classic Smagorinsky model,
   - the DLN algorithm for standard NSE.
4. We use the discrete Grönwall inequality in Lemma 2.4, approximation for Stokes projection in (10) and approximation for interpolation in (6) to achieve convergence of numerical solutions in L^2-norm and H^1-norm.

Part 1. We start with the CSM at time $t_{n,\beta}$ $(1 \le n \le N-1)$. For any $v^h \in V^h$, the variational formulation becomes

$$(w_t(t_{n,\beta}), v^h) + \frac{C_s^4\delta^2}{\mu^2}(\nabla w_t(t_{n,\beta}), \nabla v^h) + b^*\big(w(t_{n,\beta}), w(t_{n,\beta}), v^h\big) - (q(t_{n,\beta}), \nabla \cdot v^h)$$
$$+\nu(\nabla w(t_{n,\beta}), \nabla v^h) + \Big((C_s\delta)^2|\nabla w(t_{n,\beta})|\nabla w(t_{n,\beta}), \nabla v^h\Big) = \big(f(t_{n,\beta}), v^h\big),\ \forall v^h \in V^h.$$

Equivalently,

(22)
$$\begin{aligned}
&\Big(\frac{\alpha_2 w_{n+1}+\alpha_1 w_n+\alpha_0 w_{n-1}}{\widehat{k}_n}, v^h\Big) + \frac{C_s^4\delta^2}{\mu^2}\Big(\frac{\alpha_2\nabla w_{n+1}+\alpha_1\nabla w_n+\alpha_0\nabla w_{n-1}}{\widehat{k}_n}, \nabla v^h\Big)\\
&+b^*(w_{n,\beta}, w_{n,\beta}, v^h) - \big(q(t_{n,\beta}), \nabla\cdot v^h\big) + \nu(\nabla w_{n,\beta}, \nabla v^h) + \gamma(\nabla\cdot w_{n,\beta}, \nabla\cdot v^h)\\
&+\Big((C_s\delta)^2|\nabla w_{n,\beta}|\nabla w_{n,\beta}, \nabla v^h\Big)\\
&=(f_{n,\beta}, v^h) + \frac{C_s^4\delta^2}{\mu^2}\Big(\frac{\alpha_2\nabla w_{n+1}+\alpha_1\nabla w_n+\alpha_0\nabla w_{n-1}}{\widehat{k}_n} - \nabla w_t(t_{n,\beta}), \nabla v^h\Big)\\
&+\Big((C_s\delta)^2\big(|\nabla w_{n,\beta}|\nabla w_{n,\beta} - |\nabla w(t_{n,\beta})|\nabla w(t_{n,\beta})\big), \nabla v^h\Big) + \tau_n(v^h),
\end{aligned}$$

where the truncation error is

$$\begin{aligned}
\tau_n(v^h) =& \Big(\frac{\alpha_2 w_{n+1}+\alpha_1 w_n+\alpha_0 w_{n-1}}{\widehat{k}_n} - w_t(t_{n,\beta}), v^h\Big) + \nu\big(\nabla\big(w_{n,\beta} - w(t_{n,\beta})\big), \nabla v^h\big)\\
&+ b^*(w_{n,\beta}, w_{n,\beta}, v^h) - b^*(w(t_{n,\beta}), w(t_{n,\beta}), v^h) + \big(f(t_{n,\beta}) - f_{n,\beta}, v^h\big).
\end{aligned}$$

We denote the error $e_n = w_n - w_n^h$ and $e_{n,\beta} = \sum_{\ell=0}^{2}\beta_\ell^{(n)} e_{n-1+\ell}$. Then we subtract the DLN scheme in (11) from (22) to get the following error equation: $\forall v^h \in V^h$

(23)
$$\begin{aligned}
&\Big(\frac{\alpha_2 e_{n+1}+\alpha_1 e_n+\alpha_0 e_{n-1}}{\widehat{k}_n}, v^h\Big) + \frac{C_s^4\delta^2}{\mu^2}\Big(\frac{\alpha_2\nabla e_{n+1}+\alpha_1\nabla e_n+\alpha_0\nabla e_{n-1}}{\widehat{k}_n}, \nabla v^h\Big)\\
&+ b^*(w_{n,\beta}, w_{n,\beta}, v^h) - b^*(w_{n,\beta}^h, w_{n,\beta}^h, v^h) + \nu(\nabla e_{n,\beta}, \nabla v^h) + \gamma(\nabla\cdot e_{n,\beta}, \nabla\cdot v^h)\\
&+\Big((C_s\delta)^2(|\nabla w_{n,\beta}|\nabla w_{n,\beta} - |\nabla w_{n,\beta}^h|\nabla w_{n,\beta}^h), \nabla v^h\Big)\\
&=\big(q(t_{n,\beta}), \nabla\cdot v^h\big) + \frac{C_s^4\delta^2}{\mu^2}\Big(\frac{\alpha_2\nabla w_{n+1}+\alpha_1\nabla w_n+\alpha_0\nabla w_{n-1}}{\widehat{k}_n} - \nabla w_t(t_{n,\beta}), \nabla v^h\Big)\\
&+\Big((C_s\delta)^2\big(|\nabla w_{n,\beta}|\nabla w_{n,\beta} - |\nabla w(t_{n,\beta})|\nabla w(t_{n,\beta})\big), \nabla v^h\Big) + \tau_n(v^h).
\end{aligned}$$

Part 2. We denote W_n to be velocity component of Stokes projection $(w_n, 0)$ onto $V^h \times Q^h$ and denote

$$\eta_n := w_n - W_n, \qquad \phi_n^h := w_n^h - W_n.$$

Thus $e_n = \eta_n - \phi_n^h$. Notice that,

$$\begin{aligned}
&b^*(w_{n,\beta}, w_{n,\beta}, v^h) - b^*(w_{n,\beta}^h, w_{n,\beta}^h, v^h)\\
=&b^*(w_{n,\beta}, w_{n,\beta}, v^h) - b^*(w_{n,\beta}^h, w_{n,\beta}, v^h)\\
&+ b^*(w_{n,\beta}^h, w_{n,\beta}, v^h) - b^*(w_{n,\beta}^h, w_{n,\beta}^h, v^h),\\
=&b^*(e_{n,\beta}, w_{n,\beta}, v^h) + b^*(w_{n,\beta}^h, e_{n,\beta}, v^h),
\end{aligned}$$

and

$$\begin{aligned}
&\int_\Omega (|\nabla w_{n,\beta}|\nabla w_{n,\beta} - |\nabla w_{n,\beta}^h|\nabla w_{n,\beta}^h) : \nabla v^h dx\\
=&\int_\Omega (|\nabla w_{n,\beta}|\nabla w_{n,\beta} - |\nabla W_{n,\beta}|\nabla W_{n,\beta} + |\nabla W_{n,\beta}|\nabla W_{n,\beta} - |\nabla w_{n,\beta}^h|\nabla w_{n,\beta}^h) : \nabla v^h dx.
\end{aligned}$$

We also adopt the following notations

$$\eta_{n,\beta} = \sum_{\ell=0}^{2} \beta_\ell^{(n)} \eta_{n-1+\ell}, \qquad \phi_{n,\beta}^h = \sum_{\ell=0}^{2} \beta_\ell^{(n)} \phi_{n-1+\ell}^h,$$

and use the above calculations to derive the error equations from (23)

(24)

$$\begin{aligned}
&\Big(\frac{\alpha_2\phi_{n+1}^h+\alpha_1\phi_n^h+\alpha_0\phi_{n-1}^h}{\widehat{k}_n}, v^h\Big) + \frac{C_s^4\delta^2}{\mu^2}\Big(\frac{\alpha_2\nabla\phi_{n+1}^h+\alpha_1\nabla\phi_n^h+\alpha_0\nabla\phi_{n-1}^h}{\widehat{k}_n}, \nabla v^h\Big)\\
&-b^*(e_{n,\beta}, w_{n,\beta}, v^h) - b^*(w_{n,\beta}^h, e_{n,\beta}, v^h) + \nu(\nabla\phi_{n,\beta}^h, \nabla v^h) + \gamma(\nabla\cdot\phi_{n,\beta}^h, \nabla\cdot v^h)\\
&+ (C_s\delta)^2 \int_\Omega (|\nabla w_{n,\beta}^h|\nabla w_{n,\beta}^h - |\nabla W_{n,\beta}|\nabla W_{n,\beta}) : (\nabla v^h) dx\\
=&\Big(\frac{\alpha_2\eta_{n+1}+\alpha_1\eta_n+\alpha_0\eta_{n-1}}{\widehat{k}_n}, v^h\Big) + \frac{C_s^4\delta^2}{\mu^2}\Big(\frac{\alpha_2\nabla\eta_{n+1}+\alpha_1\nabla\eta_n+\alpha_0\nabla\eta_{n-1}}{\widehat{k}_n}, \nabla v^h\Big)\\
&+ (C_s\delta)^2 \int_\Omega (|\nabla w_{n,\beta}|\nabla w_{n,\beta} - |\nabla W_{n,\beta}|\nabla W_{n,\beta}) : \nabla v^h dx\\
&+ \nu(\nabla\eta_{n,\beta}, \nabla v^h) + \gamma(\nabla\cdot\eta_{n,\beta}, \nabla\cdot v^h) - \big(q(t_{n,\beta}), \nabla\cdot v^h\big)\\
&- \frac{C_s^4\delta^2}{\mu^2}\Big(\frac{\alpha_2\nabla w_{n+1} + \alpha_1\nabla w_n + \alpha_0\nabla w_{n-1}}{\widehat{k}_n} - \nabla w_t(t_{n,\beta}), \nabla v^h\Big)\\
&-\Big((C_s\delta)^2\big(|\nabla w_{n,\beta}|\nabla w_{n,\beta} - |\nabla w(t_{n,\beta})|\nabla w(t_{n,\beta})\big), \nabla v^h\Big) - \tau_n(v^h).
\end{aligned}$$

We set $v^h = \phi^h_{n,\beta}$ in (24) and use (13) in Lemma 4.2,

$$
\begin{aligned}
&\left\|\begin{matrix}\phi^h_{n+1}\\ \phi^h_n\end{matrix}\right\|^2_{G(\theta)} - \left\|\begin{matrix}\phi^h_{n}\\ \phi^h_{n-1}\end{matrix}\right\|^2_{G(\theta)} + \Big\|\sum_{\ell=0}^{2}\lambda^{(n)}_\ell \phi^h_{n-1+\ell}\Big\|^2 + \nu\widehat{k}_n\|\nabla\phi^h_{n,\beta}\|^2 + \gamma\widehat{k}_n\|\nabla\cdot\phi^h_{n,\beta}\|^2\\
&+\frac{C_s^4\delta^2}{\mu^2}\Big(\left\|\begin{matrix}\nabla\phi^h_{n+1}\\ \nabla\phi^h_n\end{matrix}\right\|^2_{G(\theta)} - \left\|\begin{matrix}\nabla\phi^h_{n}\\ \nabla\phi^h_{n-1}\end{matrix}\right\|^2_{G(\theta)} + \Big\|\sum_{\ell=0}^{2}\lambda^{(n)}_\ell\nabla\phi^h_{n-1+\ell}\Big\|^2\Big)\\
&=\frac{C_s^4\delta^2}{\mu^2}\Big(\sum_{\ell=0}^{2}\alpha_\ell\nabla\eta_{n-1+\ell},\nabla\phi^h_{n,\beta}\Big)\\
&-\frac{C_s^4\delta^2\widehat{k}_n}{\mu^2}\Big(\frac{\alpha_2\nabla w_{n+1}+\alpha_1\nabla w_n+\alpha_0\nabla w_{n-1}}{\widehat{k}_n} - \nabla w_t(t_{n,\beta}),\nabla v^h\Big)\\
&-(C_s\delta)^2\widehat{k}_n\int_\Omega(|\nabla w^h_{n,\beta}|\nabla w^h_{n,\beta} - |\nabla W_{n,\beta}|\nabla W_{n,\beta}):(\nabla\phi^h_{n,\beta})dx\\
&+(C_s\delta)^2\widehat{k}_n\int_\Omega(|\nabla w_{n,\beta}|\nabla w_{n,\beta} - |\nabla W_{n,\beta}|\nabla W_{n,\beta}):\nabla\phi^h_{n,\beta}dx\\
&-\widehat{k}_n\Big((C_s\delta)^2\big(|\nabla w_{n,\beta}|\nabla w_{n,\beta} - |\nabla w(t_{n,\beta})|\nabla w(t_{n,\beta})\big),\nabla v^h\Big)\\
&+\Big(\sum_{\ell=0}^{2}\alpha_\ell\eta_{n-1+\ell},\phi^h_{n,\beta}\Big) + \nu\widehat{k}_n(\nabla\eta_{n,\beta},\nabla\phi^h_{n,\beta}) + \gamma\widehat{k}_n(\nabla\cdot\eta_{n,\beta},\nabla\cdot\phi^h_{n,\beta})\\
&-\widehat{k}_n\big(q(t_{n,\beta}),\nabla\cdot\phi^h_{n,\beta}\big) + \widehat{k}_n b^*(e_{n,\beta},w_{n,\beta},\phi^h_{n,\beta}) + \widehat{k}_n b^*(w^h_{n,\beta},e_{n,\beta},\phi^h_{n,\beta})\\
&-\widehat{k}_n\tau_n(\phi^h_{n,\beta}).
\end{aligned}
\tag{25}
$$

On the right-hand side of equation (25), the first two terms are due to the new kinetic energy penalization in the CSM, the third to fifth terms arise from the classic Smagorinsky model, and the remaining terms are from the DLN scheme for standard NSE.

Step 3. Now we deal with the terms on the right hand side of (25).
• *The term due to the new kinetic energy penalization in the CSM:*
By Cauchy Schwarz inequality, Poincaré inequality and Young's inequality,

$$
\frac{C_s^4\delta^2}{\mu^2}\Big(\sum_{\ell=0}^{2}\alpha_\ell\nabla\eta_{n-1+\ell},\nabla\phi^h_{n,\beta}\Big) \le \frac{C}{\nu\widehat{k}_n}\Big(\frac{C_s^4\delta^2}{\mu^2}\Big)^2\Big\|\sum_{\ell=0}^{2}\alpha_\ell\nabla\eta_{n-1+\ell}\Big\|^2 + \frac{\nu\widehat{k}_n}{32}\|\nabla\phi^h_{n,\beta}\|^2.
\tag{26}
$$

We use the approximation of Stokes projection in (10), approximation theorem of interpolation in (6) and Hölder's inequality

$$
\begin{aligned}
\Big\|\sum_{\ell=0}^{2}\alpha_\ell\nabla\eta_{n-1+\ell}\Big\|^2 &\le Ch^{2r}\Big\|\sum_{\ell=0}^{2}\alpha_\ell\nabla w_{n-1+\ell}\Big\|^2_{r+1}\\
&\le C(\theta)h^{2r}\big(\|w_{n+1}-w_n\|^2_{r+1} + \|w_{n+1}-w_{n-1}\|^2_{r+1}\big)\\
&\le C(\theta)h^{2r}(k_n+k_{n-1})\int_{t_{n-1}}^{t_{n+1}}\|w_t\|^2_{r+1}dt.
\end{aligned}
\tag{27}
$$

By (27), (26) becomes

$$\frac{C_s^4\delta^2}{\mu^2}\Big(\sum_{\ell=0}^{2}\alpha_\ell\nabla\eta_{n-1+\ell},\nabla\phi_{n,\beta}^h\Big)\leq C(\theta)h^{2r}\Big(\frac{C_s^4\delta^2}{\mu^2}\Big)^2\int_{t_{n-1}}^{t_{n+1}}\|w_t\|_{r+1}^2dt+\frac{\nu\widehat{k}_n}{32}\|\nabla\phi_{n,\beta}^h\|^2. \tag{28}$$

By Cauchy-Schwarz inequality, Young's inequality and (16) in Lemma 4.4

$$\begin{aligned}&\frac{C_s^4\delta^2\widehat{k}_n}{\mu^2}\Big(\frac{\alpha_2\nabla w_{n+1}+\alpha_1\nabla w_n+\alpha_0\nabla w_{n-1}}{\widehat{k}_n}-\nabla w_t(t_{n,\beta}),\nabla\phi_{n,\beta}^h\Big)\\ \leq&\frac{C\widehat{k}_n}{\nu}\Big(\frac{C_s^4\delta^2}{\mu^2}\Big)^2\Big\|\nabla\Big(\frac{\alpha_2 w_{n+1}+\alpha_1 w_n+\alpha_0 w_{n-1}}{\widehat{k}_n}-w_t(t_{n,\beta})\Big)\Big\|^2+\frac{\nu\widehat{k}_n}{32}\|\nabla\phi_{n,\beta}^h\|^2\\ \leq&\frac{C(\theta)k_{\max}^4}{\nu}\Big(\frac{C_s^4\delta^2}{\mu^2}\Big)^2\int_{t_{n-1}}^{t_{n+1}}\|\nabla w_{ttt}\|^2dt+\frac{\nu\widehat{k}_n}{32}\|\nabla\phi_{n,\beta}^h\|^2.\end{aligned} \tag{29}$$

• *Viscous terms arising from the classic Smagorinsky model:*
By strong monotonicity property (**SM**) in Lemma 2.5,

$$\begin{aligned}&(C_s\delta)^2\widehat{k}_n\int_\Omega(|\nabla w_{n,\beta}^h|\nabla w_{n,\beta}^h-|\nabla W_{n,\beta}|\nabla W_{n,\beta}):(\nabla\phi_{n,\beta}^h)dx\\ \geq&C_1(C_s\delta)^2\widehat{k}_n\|\nabla\phi_{n,\beta}^h\|_{0,3}^3.\end{aligned} \tag{30}$$

We denote $\mathcal{R}_n=\max\{\|\nabla w_{n,\beta}\|_{0,3},\|\nabla W_{n,\beta}\|_{0,3}\}$ and use Local Lipschitz continuity (**LLC**) in Lemma 2.5

$$\begin{aligned}&(C_s\delta)^2\widehat{k}_n\int_\Omega(|\nabla w_{n,\beta}|\nabla w_{n,\beta}-|\nabla W_{n,\beta}|\nabla W_{n,\beta}):(\nabla\phi_{n,\beta}^h)dx\\ \leq&(C_s\delta)^2\widehat{k}_nC_2\mathcal{R}_n\|\nabla\eta_{n,\beta}\|_{0,3}\|\nabla\phi_{n,\beta}^h\|_{0,3}\\ \leq&\frac{C(C_s\delta)^2C_2^{3/2}\widehat{k}_n}{\sqrt{C_1}}\mathcal{R}_n^{3/2}\|\nabla\eta_{n,\beta}\|_{0,3}^{3/2}+\frac{C_1(C_s\delta)^2\widehat{k}_n}{3}\|\nabla\phi_{n,\beta}^h\|_{0,3}^3.\end{aligned}$$

By triangle inequality,

$$\mathcal{R}_n\leq\max\big\{\|\nabla w_{n,\beta}\|_{0,3},\big\|\nabla\big(W_{n,\beta}-w_{n,\beta}\big)\big\|_{0,3}+\|\nabla w_{n,\beta}\|_{0,3}\big\}=\|\nabla\eta_{n,\beta}\|_{0,3}+\|\nabla w_{n,\beta}\|_{0,3}.$$

We use (7) in Theorem 2.6, the bound for Stokes projection in (10) and approximation theorem of interpolation in (6)

$$\|\nabla\eta_{n,\beta}\|_{0,3}\leq Ch^{-d/6}\|\nabla\eta_{n,\beta}\|\leq Ch^{r-d/6}\|w_{n,\beta}\|_{r+1}.$$

By the fact: for any $a,b,c\in\mathbb{R}$ with $c>1$,

$$(|a|+|b|)^c\leq 2^{c-1}(|a|^c+|b|^c), \tag{31}$$

we have

$$\begin{aligned}\mathcal{R}_n^{3/2}\|\nabla\eta_{n,\beta}\|_{0,3}^{3/2}\leq&C\big(\|\nabla\eta_{n,\beta}\|_{0,3}^3+\|\nabla\eta_{n,\beta}\|_{0,3}^{3/2}\|\nabla w_{n,\beta}\|_{0,3}^{3/2}\big)\\ \leq&Ch^{3r-d/2}\|w_{n,\beta}\|_{r+1}^3+Ch^{3/2r-d/4}\|w_{n,\beta}\|_{r+1}^{3/2}\|\nabla w_{n,\beta}\|_{0,3}^{3/2}\\ \leq&Ch^{3r-d/2}\|w_{n,\beta}\|_{r+1}^3+Ch^{3/2r-d/4}\big(\|w_{n,\beta}\|_{r+1}^3+\|\nabla w_{n,\beta}\|_{0,3}^3\big).\end{aligned} \tag{32}$$

By triangle inequality, the fact in (31), (16) in Lemma 4.4 and Hölder's inequality,

$$
\begin{aligned}
\|w_{n,\beta}\|_{r+1}^3 \leq & C\|w_{n,\beta}-w(t_{n,\beta})\|_{r+1}^3 + C\|w(t_{n,\beta})\|_{r+1}^3 \\
\leq & C\Big(k_{\max}^3\int_{t_{n-1}}^{t_{n+1}}\|w_{tt}\|_{r+1}^2dt\Big)^{3/2} + C\|w(t_{n,\beta})\|_{r+1}^3 \\
\leq & Ck_{\max}^5\int_{t_{n-1}}^{t_{n+1}}\|w_{tt}\|_{r+1}^3dt + C\|w(t_{n,\beta})\|_{r+1}^3.
\end{aligned} \tag{33}
$$

By (32) and (33), (31) becomes

$$
\begin{aligned}
&(C_s\delta)^2\widehat{k}_n\int_\Omega(|\nabla w_{n,\beta}|\nabla w_{n,\beta}-|\nabla W_{n,\beta}|\nabla W_{n,\beta}):(\nabla\phi_{n,\beta}^h)dx \\
\leq & \frac{C(C_s\delta)^2C_2^{\frac{3}{2}}}{\sqrt{C_1}}\Big[(1+h^{\frac{3r}{2}-\frac{d}{4}})h^{\frac{3r}{2}-\frac{d}{4}}\big(k_{\max}^6\int_{t_{n-1}}^{t_{n+1}}\|w_{tt}\|_{r+1}^3dt+(k_n+k_{n-1})\|w(t_{n,\beta})\|_{r+1}^3\big) \\
& + h^{\frac{3r}{2}-\frac{d}{4}}\big(k_{\max}^6\int_{t_{n-1}}^{t_{n+1}}\|\nabla w_{tt}\|_{0,3}^3dt + (k_n+k_{n-1})\|\nabla w(t_{n,\beta})\|_{0,3}^3\big)\Big].
\end{aligned} \tag{34}
$$

We denote $\mathcal{S}_n = \max\big\{\|\nabla w_{n,\beta}\|_{0,3}, \|\nabla w(t_{n,\beta})\|_{0,3}\big\}$. By (**LLC**) in Lemma 2.5 and Young's inequality,

$$
\begin{aligned}
&\widehat{k}_n\Big((C_s\delta)^2(|\nabla w_{n,\beta}|\nabla w_{n,\beta}-|\nabla w(t_{n,\beta})|\nabla w(t_{n,\beta})),\nabla\phi_{n,\beta}^h\Big) \\
\leq & \widehat{k}_n(C_s\delta)^2C_2\mathcal{S}_n\big\|\nabla(w_{n,\beta}-w(t_{n,\beta}))\big\|_{0,3}\|\nabla\phi_{n,\beta}^h\|_{0,3} \\
\leq & \frac{C(C_s\delta)^2C_2^{3/2}\widehat{k}_n}{\sqrt{C_1}}\mathcal{S}_n^{3/2}\big\|\nabla(w_{n,\beta}-w(t_{n,\beta}))\big\|_{0,3}^{3/2} + \frac{C_1(C_s\delta)^2\widehat{k}_n}{4}\|\nabla\phi_{n,\beta}^h\|_{0,3}^3.
\end{aligned} \tag{35}
$$

By (16) in Lemma 4.4 and Young's inequality,

$$
\begin{aligned}
&\mathcal{S}_n^{\frac{3}{2}}\big\|\nabla\big(w(t_{n,\beta})-w_{n,\beta}\big)\big\|_{0,3}^{\frac{3}{2}} \\
\leq & C\Big(\big\|\nabla\big(w(t_{n,\beta})-w_{n,\beta}\big)\big\|_{0,3}^3+\big\|\nabla\big(w(t_{n,\beta})-w_{n,\beta}\big)\big\|_{0,3}^{\frac{3}{2}}\|\nabla w_{n,\beta}\|_{0,3}^{\frac{3}{2}}\Big) \\
\leq & C(\theta)\Big(k_{\max}^3\int_{t_{n-1}}^{t_{n+1}}\|\nabla w_{tt}\|_{0,3}^2dt\Big)^{\frac{3}{2}}+C(\theta)\Big(k_{\max}^3\int_{t_{n-1}}^{t_{n+1}}\|\nabla w_{tt}\|_{0,3}^2dt\Big)^{\frac{3}{4}}\|\nabla w_{n,\beta}\|_{0,3}^{\frac{3}{2}} \\
\leq & C(\theta)k_{\max}^{9/2}\Big(\int_{t_{n-1}}^{t_{n+1}}\|\nabla w_{tt}\|_{0,3}^2dt\Big)^{\frac{3}{2}} + C(\theta)k_{\max}^{\frac{3}{2}}\Big(\int_{t_{n-1}}^{t_{n+1}}\|\nabla w_{tt}\|_{0,3}^2dt\Big)^{\frac{3}{2}} \\
& + C(\theta)k_{\max}^3\|\nabla w_{n,\beta}\|_{0,3}^3 \\
\leq & C(\theta)k_{\max}^{\frac{9}{2}}\Big(\int_{t_{n-1}}^{t_{n+1}}\|\nabla w_{tt}\|_{0,3}^2dt\Big)^{\frac{3}{2}} + C(\theta)k_{\max}^{\frac{3}{2}}\Big(\int_{t_{n-1}}^{t_{n+1}}\|\nabla w_{tt}\|_{0,3}^2dt\Big)^{\frac{3}{2}} \\
& + C(\theta)k_{\max}^3\Big(\big\|\nabla\big(w(t_{n,\beta})-w_{n,\beta}\big)\big\|_{0,3}^3+\|\nabla w(t_{n,\beta})\|_{0,3}^3\Big) \\
\leq & C(\theta)\big(k_{\max}^{\frac{15}{2}}+k_{\max}^{\frac{9}{2}}+k_{\max}^{\frac{3}{2}}\big)\Big(\int_{t_{n-1}}^{t_{n+1}}\|\nabla w_{tt}\|_{0,3}^2dt\Big)^{\frac{3}{2}}+C(\theta)k_{\max}^3\|\nabla w(t_{n,\beta})\|_{0,3}^3.
\end{aligned} \tag{36}
$$

By Hölder's inequality,

$$
\Big(\int_{t_{n-1}}^{t_{n+1}}\|\nabla w_{tt}\|_{0,3}^2dt\Big)^{3/2} \leq Ck_{\max}^{1/2}\int_{t_{n-1}}^{t_{n+1}}\|\nabla w_{tt}\|_{0,3}^3dt. \tag{37}
$$

By (36) and (37), (35) becomes

$$\begin{aligned}&\widehat{k}_n\Big((C_s\delta)^2(|\nabla w_{n,\beta}|\nabla w_{n,\beta}-|\nabla w(t_{n,\beta})|\nabla w(t_{n,\beta})),\nabla\phi^h_{n,\beta}\Big)\\ \leq&\frac{C(\theta)k_{\max}^3(C_s\delta)^2C_2^{3/2}}{\sqrt{C_1}}\Big[\big(k_{\max}^6+k_{\max}^3+1\big)\int_{t_{n-1}}^{t_{n+1}}\|\nabla w_{tt}\|_{0,3}^3dt\\ &+(k_n+k_{n-1})\|\nabla w(t_{n,\beta})\|_{0,3}^3\Big].\end{aligned}\tag{38}$$

• *Terms coming from the DLN scheme for standard NSE:*
Similar to the treatment of (28), we have

$$\Big(\sum_{\ell=0}^{2}\alpha_\ell\eta_{n-1+\ell},\phi^h_{n,\beta}\Big)\leq C(\theta)h^{2r+2}\int_{t_{n-1}}^{t_{n+1}}\|w_t\|_{r+1}^2dt+\frac{\nu\widehat{k}_n}{32}\|\nabla\phi^h_{n,\beta}\|^2.\tag{39}$$

By the definition of Stokes projection in (9), $(\nabla\eta_{n,\beta},\nabla\phi^h_{n,\beta})=0$. By Cauchy Schwarz inequality, Poincaré inequality and Young's inequality,

$$\begin{aligned}\gamma\widehat{k}_n(\nabla\cdot\eta_{n,\beta},\nabla\cdot\phi^h_{n,\beta})\leq&\gamma d\widehat{k}_n\|\nabla\eta_{n,\beta}\|\|\nabla\phi^h_{n,\beta}\|\\ \leq&\frac{C\gamma^2\widehat{k}_n}{\nu}\|\nabla\eta_{n,\beta}\|^2+\frac{\nu\widehat{k}_n}{32}\|\nabla\phi^h_{n,\beta}\|^2.\end{aligned}\tag{40}$$

By the approximation of Stokes projection in (10), triangle inequality and (16) in Lemma 4.4

$$\begin{aligned}\|\nabla\eta_{n,\beta}\|^2\leq&Ch^{2r}\big(\|w_{n,\beta}-w(t_{n,\beta})\|_{r+1}^2+\|w(t_{n,\beta})\|_{r+1}^2\big)\\ \leq&Ch^{2r}\Big(k_{\max}^3\int_{t_{n-1}}^{t_{n+1}}\|w_{tt}\|_{r+1}^2dt+\|w(t_{n,\beta})\|_{r+1}^2\Big).\end{aligned}\tag{41}$$

By (41), (40) becomes

$$\begin{aligned}&\gamma\widehat{k}_n(\nabla\cdot\eta_{n,\beta},\nabla\cdot\phi^h_{n,\beta})\\ \leq&\frac{C\gamma^2h^{2r}}{\nu}\Big(k_{\max}^4\int_{t_{n-1}}^{t_{n+1}}\|w_{tt}\|_{r+1}^2dt+(k_n+k_{n-1})\|w(t_{n,\beta})\|_{r+1}^2\Big)+\frac{\nu\widehat{k}_n}{32}\|\nabla\phi^h_{n,\beta}\|^2.\end{aligned}\tag{42}$$

We choose p^h to be L^2-projection of $q(t_{n,\beta})$ onto Q^h, then

$$\widehat{k}_n\big(q(t_{n,\beta}),\nabla\cdot\phi^h_{n,\beta}\big)=\widehat{k}_n\big(q(t_{n,\beta})-p^h,\nabla\cdot\phi^h_{n,\beta}\big)\leq\sqrt{d\widehat{k}_n}\|q(t_{n,\beta})-p^h\|\|\nabla\phi^h_{n,\beta}\|.$$

By Young's inequality and approximation of pressure in (6), we have

$$\widehat{k}_n\big(q(t_{n,\beta}),\nabla\cdot\phi^h_{n,\beta}\big)\leq\frac{Ch^{2s+2}}{\nu}(k_n+k_{n-1})\|q(t_{n,\beta})\|_{s+1}^2+\frac{\nu\widehat{k}_n}{32}\|\nabla\phi^h_{n,\beta}\|^2.\tag{43}$$

By (4) in Lemma 2.3, Young's inequality and approximation of Stokes projection in (6)

$$\begin{aligned}&\widehat{k}_nb^*(e_{n,\beta},w_{n,\beta},\phi^h_{n,\beta})\\ =&\widehat{k}_nb^*(\eta_{n,\beta},w_{n,\beta},\phi^h_{n,\beta})-\widehat{k}_nb^*(\phi^h_{n,\beta},w_{n,\beta},\phi^h_{n,\beta})\\ \leq&C\widehat{k}_n\|\nabla\eta_{n,\beta}\|\|\nabla w_{n,\beta}\|\|\nabla\phi^h_{n,\beta}\|+C\widehat{k}_n\|\phi^h_{n,\beta}\|^{1/2}\|\nabla w_{n,\beta}\|\|\nabla\phi^h_{n,\beta}\|^{3/2}\\ \leq&\frac{C\widehat{k}_n}{\nu}\|\nabla\eta_{n,\beta}\|^2\|\nabla w_{n,\beta}\|^2+\frac{C\widehat{k}_n}{\nu^3}\|\nabla w_{n,\beta}\|^4\|\phi^h_{n,\beta}\|^2+\frac{\nu\widehat{k}_n}{32}\|\nabla\phi^h_{n,\beta}\|^2\\ \leq&\frac{C\widehat{k}_nh^{2r}}{\nu}\big(\|w_{n,\beta}\|_{r+1}^4+\|\nabla w_{n,\beta}\|^4\big)+\frac{C\widehat{k}_n}{\nu^3}\|\nabla w_{n,\beta}\|^4\|\phi^h_{n,\beta}\|^2+\frac{\nu\widehat{k}_n}{32}\|\nabla\phi^h_{n,\beta}\|^2.\end{aligned}\tag{44}$$

We use triangle inequality, (16) in Lemma 4.4 and Hölder's inequality

$$\begin{aligned}\|w_{n,\beta}\|_{r+1}^4 \leq& C\big(\|w_{n,\beta}-w(t_{n,\beta})\|_{r+1}^4+\|w(t_{n,\beta})\|_{r+1}^4\big)\\ \leq& C\Big[\big(Ck_{\max}^3\int_{t_{n-1}}^{t_{n+1}}1\cdot\|w_{tt}\|_{r+1}^2dt\big)^2+\|w(t_{n,\beta})\|_{r+1}^4\Big]\\ \leq& C(\theta)\Big(k_{\max}^7\int_{t_{n-1}}^{t_{n+1}}\|w_{tt}\|_{r+1}^4dt+\|w(t_{n,\beta})\|_{r+1}^4\Big),\\ \|\nabla w_{n,\beta}\|^4 \leq& C(\theta)\Big(k_{\max}^7\int_{t_{n-1}}^{t_{n+1}}\|\nabla w_{tt}\|^4dt+\|\nabla w(t_{n,\beta})\|^4\Big).\end{aligned}$$

Thus (44) becomes

$$\begin{aligned}&\widehat{k}_n b^*(e_{n,\beta},w_{n,\beta},\phi_{n,\beta}^h)\\ \leq&\frac{C(\theta)h^{2r}}{\nu}\Big(k_{\max}^8\int_{t_{n-1}}^{t_{n+1}}\|w_{tt}\|_{r+1}^4dt+k_{\max}^8\int_{t_{n-1}}^{t_{n+1}}\|\nabla w_{tt}\|^4dt\\ &+(k_n+k_{n-1})\|w(t_{n,\beta})\|_{r+1}^4+(k_n+k_{n-1})\|\nabla w(t_{n,\beta})\|^4\Big)\\ &+\frac{C\widehat{k}_n}{\nu^3}\|\nabla w_{n,\beta}\|^4\|\phi_{n,\beta}^h\|^2+\frac{\nu\widehat{k}_n}{32}\|\nabla\phi_{n,\beta}^h\|^2.\end{aligned}\tag{45}$$

By (3), (4), approximation of Stokes projection in (10) and approximation theorem for interpolation in (6)

$$\begin{aligned}\widehat{k}_n b^*(w_{n,\beta}^h,e_{n,\beta},\phi_{n,\beta}^h)\leq&\frac{C\widehat{k}_n}{\nu}\|\nabla w_{n,\beta}^h\|^2\|\nabla\eta_{n,\beta}\|^2+\frac{\nu\widehat{k}_n}{32}\|\nabla\phi_{n,\beta}^h\|^2\\ \leq&\frac{Ch^r\widehat{k}_n}{\nu}|||w|||_{\infty,r+1,2}^2\|\nabla w_{n,\beta}^h\|^2+\frac{\nu\widehat{k}_n}{32}\|\nabla\phi_{n,\beta}^h\|^2.\end{aligned}\tag{46}$$

Now we deal with $\widehat{k}_n\tau_n(\phi_{n,\beta}^h)$: by Cauchy Schwarz inequality, Poincaré inequality and (16) in Lemma 4.4, the first three terms become

$$\begin{aligned}&\widehat{k}_n\Big(\frac{\alpha_2w_{n+1}+\alpha_1w_n+\alpha_0w_{n-1}}{\widehat{k}_n}-w_t(t_{n,\beta}),\phi_{n,\beta}^h\Big)\\ \leq&C\widehat{k}_n\Big\|\frac{\alpha_2w_{n+1}+\alpha_1w_n+\alpha_0w_{n-1}}{\widehat{k}_n}-w_t(t_{n,\beta})\Big\|\|\nabla\phi_{n,\beta}^h\|\\ \leq&\frac{C\widehat{k}_n}{\nu}\Big\|\frac{\alpha_2w_{n+1}+\alpha_1w_n+\alpha_0w_{n-1}}{\widehat{k}_n}-w_t(t_{n,\beta})\Big\|^2+\frac{\nu\widehat{k}_n}{32}\|\nabla\phi_{n,\beta}^h\|^2\\ \leq&\frac{C(\theta)k_{\max}^4}{\nu}\int_{t_{n-1}}^{t_{n+1}}\|w_{ttt}\|^2dt+\frac{\nu\widehat{k}_n}{32}\|\nabla\phi_{n,\beta}^h\|^2,\end{aligned}\tag{47}$$

$$\begin{aligned}&\widehat{\nu k_n}\big(\nabla(w_{n,\beta}-w(t_{n,\beta})),\nabla\phi_{n,\beta}^h\big)\\ \leq&\frac{C\widehat{k}_n}{\nu}\big\|\nabla w_{n,\beta}-\nabla w(t_{n,\beta})\big\|+\frac{\nu\widehat{k}_n}{32}\|\nabla\phi_{n,\beta}^h\|^2\\ \leq&\frac{Ck_{\max}^4}{\nu}\int_{t_{n-1}}^{t_{n+1}}\|\nabla w_{tt}\|^2dt+\frac{\nu\widehat{k}_n}{32}\|\nabla\phi_{n,\beta}^h\|^2.\end{aligned}\tag{48}$$

By (4) in Lemma 2.3 and triangle inequality, two non-linear terms become

$$\begin{aligned}
&\widehat{k}_n b^*\big(w_{n,\beta}, w_{n,\beta}, \phi^h_{n,\beta}\big) - \widehat{k}_n b^*\big(w(t_{n,\beta}), w(t_{n,\beta}), \phi^h_{n,\beta}\big)\\
=&\widehat{k}_n b^*\big(w_{n,\beta} - w(t_{n,\beta}), w_{n,\beta}, \phi^h_{n,\beta}\big) + \widehat{k}_n b^*\big(w(t_{n,\beta}), w_{n,\beta} - w(t_{n,\beta}), \phi^h_{n,\beta}\big)\\
\le&\frac{C\widehat{k}_n}{\nu}\big\|\nabla(w_{n,\beta} - w(t_{n,\beta}))\big\|^2\big(\|\nabla w_{n,\beta}\|^2 + \|\nabla w(t_{n,\beta})\|^2\big) + \frac{\nu\widehat{k}_n}{32}\|\nabla\phi^h_{n,\beta}\|^2\\
\le&\frac{C\widehat{k}_n}{\nu}\big\|\nabla(w_{n,\beta}-w(t_{n,\beta}))\big\|^2\big(\big\|\nabla(w_{n,\beta}-w(t_{n,\beta}))\big\|^2+2\|\nabla w(t_{n,\beta})\|^2\big)+\frac{\nu\widehat{k}_n}{32}\|\nabla\phi^h_{n,\beta}\|^2.
\end{aligned}$$

By (16) in Lemma 4.4 and Hölder's inequality,

$$\begin{aligned}
\big\|\nabla(w_{n,\beta} - w(t_{n,\beta}))\big\|^4 \le& C(\theta)k^7_{\max}\int_{t_{n-1}}^{t_{n+1}}\|\nabla w_{tt}\|^4 dt.\\
\big\|\nabla(w_{n,\beta}-w(t_{n,\beta}))\big\|^2\|\nabla w(t_{n,\beta})\|^2 \le& C(\theta)k^3_{\max}\int_{t_{n-1}}^{t_{n+1}}\|\nabla w(t_{n,\beta})\|^2\|\nabla w_{tt}\|^2 dt\\
\le& C(\theta)k^3_{\max}\int_{t_{n-1}}^{t_{n+1}}\big(\|\nabla w(t_{n,\beta})\|^4+\|\nabla w_{tt}\|^4\big)dt\\
\le& C(\theta)k^3_{\max}\int_{t_{n-1}}^{t_{n+1}}\|\nabla w_{tt}\|^4 dt+C(\theta)k^4_{\max}\|\nabla w(t_{n,\beta})\|^4.
\end{aligned}$$

Hence,

$$\begin{aligned}
&\widehat{k}_n b^*\big(w_{n,\beta}, w_{n,\beta}, \phi^h_{n,\beta}\big)-\widehat{k}_n b^*\big(w(t_{n,\beta}), w(t_{n,\beta}), \phi^h_{n,\beta}\big)\\
\le&\frac{C(\theta)k^4_{\max}}{\nu}\Big[\big(1+k^4_{\max}\big)\int_{t_{n-1}}^{t_{n+1}}\|\nabla w_{tt}\|^4 dt+(k_n+k_{n-1})\|\nabla w(t_{n,\beta})\|^4\Big]+\frac{\nu\widehat{k}_n}{32}\|\nabla\phi^h_{n,\beta}\|^2.
\end{aligned}\tag{49}$$

By Cauchy-Schwarz inequality, Poincaré inequality, Young's inequality and (16) in Lemma 4.4

$$\begin{aligned}
\widehat{k}_n\big(f(t_{n,\beta}) - f_{n,\beta}, \phi^h_{n,\beta}\big) \le& \frac{C\widehat{k_n}}{\nu}\|f(t_{n,\beta}) - f_{n,\beta}\|^2_{-1} + \frac{\nu\widehat{k}_n}{32}\|\nabla\phi^h_{n,\beta}\|^2\\
\le& \frac{C\widehat{k}_n}{\nu}k^3_{\max}\int_{t_{n-1}}^{t_{n+1}}\|f_{tt}\|^2_{-1}dt + \frac{\nu\widehat{k}_n}{32}\|\nabla\phi^h_{n,\beta}\|^2.
\end{aligned}\tag{50}$$

Step 4.
We combine (28) - (30), (34), (38), (39), (42), (43), (45) - (50) into (25) and then sum (25) over n from 1 to $N-1$ to obtain

$$\begin{aligned}
&\left\|\begin{matrix}\phi^h_N\\ \phi^h_{N-1}\end{matrix}\right\|^2_{G(\theta)}+\frac{C_s^4\delta^2}{\mu^2}\left\|\begin{matrix}\nabla\phi^h_N\\ \nabla\phi^h_{N-1}\end{matrix}\right\|^2_{G(\theta)}+\sum_{n=1}^{N-1}\Big(\Big\|\sum_{\ell=0}^{2}\lambda^{(n)}_\ell\phi^h_{n-1+\ell}\Big\|^2+\Big\|\sum_{\ell=0}^{2}\lambda^{(n)}_\ell\nabla\phi^h_{n-1+\ell}\Big\|^2\Big)\\
&+\sum_{n=1}^{N-1}\frac{\nu}{2}\widehat{k}_n\|\nabla\phi^h_{n,\beta}\|^2+\sum_{n=1}^{N-1}\gamma\widehat{k}_n\|\nabla\cdot\phi^h_{n,\beta}\|^2+\sum_{n=1}^{N-1}C_1(C_s\delta)^2\widehat{k}_n\|\nabla\phi^h_{n,\beta}\|^3_{0,3}\\
&\le\sum_{n=1}^{N-1}\frac{C(\theta)\widehat{k}_n\|\nabla w_{n,\beta}\|^4}{\nu^3}\big(\|\phi^h_{n+1}\|^2+\|\phi^h_n\|^2+\|\phi^h_{n-1}\|^2\big)+\left\|\begin{matrix}\phi^h_1\\ \phi^h_0\end{matrix}\right\|^2_{G(\theta)}+\frac{C_s^4\delta^2}{\mu^2}\left\|\begin{matrix}\nabla\phi^h_1\\ \nabla\phi^h_0\end{matrix}\right\|^2_{G(\theta)}\\
&+\frac{Ch^r}{\nu^2}|||w|||^2_{\infty,r+1,2}\Big(\sum_{n=1}^{N-1}\nu\widehat{k}_n\|\nabla w^h_{n,\beta}\|^2\Big)+F(\theta,k_{\max},h,\delta),
\end{aligned}\tag{51}$$

where

$$
\begin{aligned}
&F(\theta, k_{\max}, h, \delta)\\
&= C(\theta)h^{2r+2}\|w_t\|^2_{L^2(0,T;H^{r+1})} + C(\theta)\Big(\frac{C_s^4\delta^2}{\mu^2}\Big)^2 h^{2r}\|w_t\|^2_{L^2(0,T;H^{r+1})}\\
&+\frac{C\gamma^2 h^{2r}}{\nu}\Big(k_{\max}^4\|w_{tt}\|^2_{L^2(0,T;H^{r+1})} + |||w|||^2_{2,r+1,2,\beta}\Big)\\
&+\frac{C(\theta)h^{2r}}{\nu}\Big(k_{\max}^8\|w_{tt}\|^4_{L^4(0,T;H^{r+1})}+k_{\max}^8\|\nabla w_{tt}\|^4_{L^4(0,T;L^2)}+|||w|||^4_{4,r+1,2,\beta}+|||\nabla w|||^4_{4,0,2,\beta}\Big)\\
&+\frac{C(C_s\delta)^2C_2^{3/2}}{\sqrt{C_1}}\Big[(1+h^{\frac{3r}{2}-\frac{d}{4}})h^{\frac{3r}{2}-\frac{d}{4}}\big(k_{\max}^6\|w_{tt}\|^3_{L^3(0,T;H^{r+1})} + |||w|||^3_{3,r+1,2,\beta}\big)\\
&+h^{\frac{3r}{2}-\frac{d}{4}}\big(k_{\max}^6\|\nabla w_{tt}\|^3_{L^3(0,T;L^3)} + |||\nabla w|||^3_{3,0,3,\beta}\big)\Big]\\
&+\frac{Ch^{2s+2}}{\nu}|||q|||^2_{2,s+1,2,\beta} + \frac{C(\theta)k_{\max}^4}{\nu}\|w_{ttt}\|^2_{L^2(0,T;L^2)} + \frac{Ck_{\max}^4}{\nu}\|\nabla w_{tt}\|^2_{L^2(0,T;L^2)}\\
&+\frac{C(\theta)k_{\max}^4}{\nu}\Big(\frac{C_s^4\delta^2}{\mu^2}\Big)^2\|\nabla w_{ttt}\|^2_{L^2(0,T;L^2)}\\
&+\frac{C(\theta)k_{\max}^4}{\nu}\Big[\big(1+k_{\max}^4\big)\|\nabla w_{tt}\|^4_{L^4(0,T;L^2)} + |||\nabla w|||^4_{4,0,2,\beta}\Big] + \frac{Ck_{\max}^4}{\nu}\|f_{tt}\|^2_{L^2(0,T;X')}\\
&+\frac{C(\theta)k_{\max}^3(C_s\delta)^2C_2^{3/2}}{\sqrt{C_1}}\Big[\big(k_{\max}^6+k_{\max}^3+1\big)\|\nabla w_{tt}\|^3_{L^3(0,T;L^3)} + |||\nabla w|||^3_{3,0,3,\beta}\Big].
\end{aligned}
$$

By (17) in Theorem 4.5,

$$\sum_{n=1}^{N-1}\nu\widehat{k}_n\|\nabla w^h_{n,\beta}\|^2 < C(\theta).$$

We set

$$D_n = \frac{C(\theta)\widehat{k}_n\|\nabla w_{n,\beta}\|^4}{k_{\max}\nu^3}, \qquad 1\le n\le N-1,$$

and

$$d_n = \begin{cases} D_1 & n=0\\ D_1+D_2 & n=1\\ D_{n-1}+D_n+D_{n+1} & 2\le n\le N-2\\ D_{N-2}+D_{N-1} & n=N-1\\ D_{N-1} & n=N\end{cases}. \tag{52}$$

By the time step restriction in (20), we have $k_{\max}d_n < 1$ for all n. Then we use the definition of $G(\theta)$-norm in (14) and apply Grönwall's inequality in Lemma 2.4 to (51) (with d_n defined in (52) and $\Delta t = k_{\max}$)

$$
\begin{aligned}
&\|\phi_N^h\|^2 + C(\theta)\sum_{n=1}^{N-1}\frac{\nu}{2}\widehat{k}_n\|\nabla\phi^h_{n,\beta}\|^2\\
&\le \exp\Big(\sum_{n=1}^{N-1}\frac{k_{\max}d_n}{1-k_{\max}d_n}\Big)\Big[\frac{C(\theta)h^r}{\nu^2}|||w|||^2_{\infty,r+1,2} + F(\theta,k_{\max},h,\delta)\\
&\quad + C(\theta)\big(\|\phi_1^h\|^2+\|\phi_0^h\|\big) + \frac{C(\theta)C_s^4\delta^2}{\mu^2}\big(\|\nabla\phi_1^h\|^2+\|\nabla\phi_0^h\|\big)\Big].
\end{aligned}
$$

By triangle inequality, approximation properties of Stokes projection in (10) and approximations of finite element space in (6), we have (21). □

Remark 4.10. *The Semi-implicit DLN algorithm has been applied to the Navier Stokes equation [53] and outperforms the corresponding fully implicit algorithm in two aspects: removing the time step restriction like* (20) *as well as avoiding the non-linear solver at each time step. For error analysis of the semi-implicit DLN algorithm for CSM* (12)*, the SM* (**SM**) *and LLC* (**LLC**) *conclusions should be adjusted and are left as an open problem. To do so, one can follow the work in [30, 31] where a new linear extrapolation of the convecting velocity for CNLE is proposed that ensures energetic stability without a time-step restriction.*

5. Numerical Tests

We perform two numerical tests in this section. The first test with known exact solutions is to verify the rate of convergence of the DLN scheme. The second test is to show that DLN exhibits intermittent backscatter under both uniform time grids and variable time steps. For both tests, we choose three values for the parameter θ: $2/3, 2/\sqrt{5}, 1$. The value $\theta = 2/3$ is proposed in [19] to minimize the error constant and maintain stability. the value $\theta = 2/\sqrt{5}$ is suggested in [40, 41] to guarantee the best stability at infinity (long-time simulations in practice). The DLN method with $\theta = 1$ is reduced to one-leg midpoint rule, having the smallest error constant [8] and conserving all quadratic Hamiltonians. We use the software FreeFem++ for programming and Taylor-Hood ($\mathbb{P}2 - \mathbb{P}1$) finite element space for spatial discretization.

5.1. A test with exact solution. We choose the test problem proposed by Guermond, Minev, and Shen [23] to confirm the second-order convergence of the constant time-stepping DLN method. The exact solutions on the domain $\Omega = (-1, 1)^2$ are

$$w(x, y, t) = \pi \sin t[\sin 2\pi y \sin^2 \pi x, -\sin 2\pi x \sin^2 \pi y]^{\mathrm{tr}},$$
$$p(x, y, t) = \sin t \cos \pi x \sin \pi y.$$

Initial conditions, boundary conditions, and body force $f(x, t)$ are decided by the exact solutions. We set model parameters $C_s = 0.1$, $\mu = 0.4$, $Re = 5000$, and δ to be the shortest edge of all triangles. We simulate the test up to $T = 10$. We denote the error of velocity and pressure at time t_n to be e_n^w and e_n^p respectively and measure the performance by the following variables

$$|||e^w|||_{\infty,0} := \max_{0\le n\le N} \|e_n^w\|_{L^2(\Omega)}, \quad |||e^w|||_{0,0} := \Big(\sum_{0\le n\le N} k\|e_n^w\|^2_{L^2(\Omega)} \Big)^{1/2},$$
$$|||e^p|||_{\infty,0} := \max_{0\le n\le N} \|e_n^p\|_{L^2(\Omega)}, \quad |||e^p|||_{0,0} := \Big(\sum_{0\le n\le N} k\|e_n^p\|^2_{L^2(\Omega)} \Big)^{1/2},$$

where k is the constant time step. From Tables 1 and 2, we observe that the constant time-stepping DLN method with $\theta = 2/3$ obtains second convergence for this test. The results of $\theta = 2/\sqrt{5}$ and $\theta = 1$ (in Tables 4 to 7) are very close thus we leave them to Appendix.

TABLE 1. Errors by $\|\cdot\|_{\infty,0}$-norm and Convergence Rate for the constant DLN with $\theta = 2/3$.

k	h	$\|\|\|e^w\|\|\|_{\infty,0}$	Rate	$\|\|\|\nabla e^w\|\|\|_{\infty,0}$	Rate	$\|\|\|e^p\|\|\|_{\infty,0}$	Rate
0.08	0.08571	6.0302	-	56.8481	-	10.8576	-
0.04	0.04221	0.0498844	6.9175	1.35745	5.3881	0.079143	7.1000
0.02	0.02095	0.0119835	2.0575	0.399758	1.7637	0.0192928	2.0364
0.01	0.01048	0.00297779	2.0087	0.10394	1.9434	0.00490525	1.9757

TABLE 2. Errors by $\|\cdot\|_{0,0}$-norm and Convergence Rate for the constant DLN with $\theta = 2/3$.

k	h	$\|\|\|e^w\|\|\|_{0,0}$	Rate	$\|\|\|\nabla e^w\|\|\|_{0,0}$	Rate	$\|\|\|e^p\|\|\|_{0,0}$	Rate
0.08	0.08571	7.8961	-	79.3971	-	12.3373	-
0.04	0.04221	0.107395	6.2001	3.06024	4.6974	0.143315	6.4277
0.02	0.02095	0.024972	2.1045	0.900864	1.7643	0.0345612	2.0520
0.01	0.01048	0.00617647	2.0155	0.234349	1.9427	0.00877951	1.9769

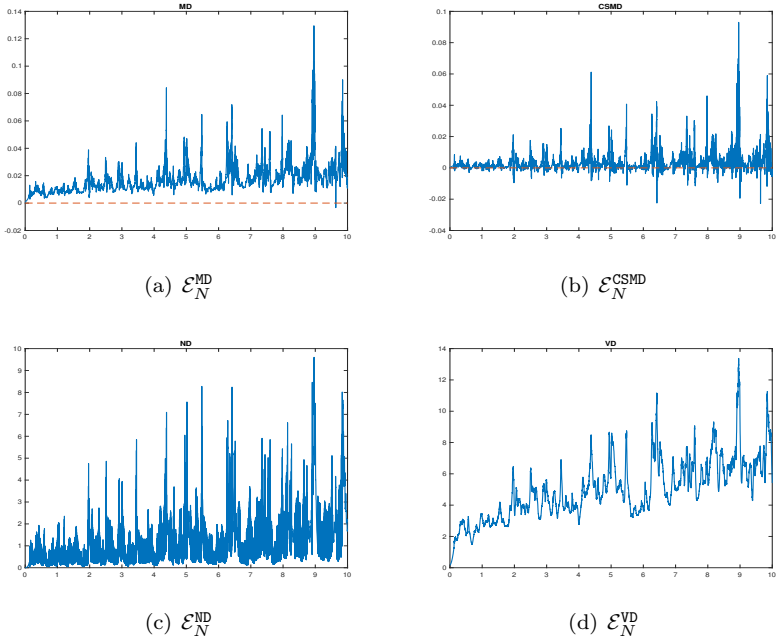

(a) $\mathcal{E}_N^{\mathtt{MD}}$ (b) $\mathcal{E}_N^{\mathtt{CSMD}}$

(c) $\mathcal{E}_N^{\mathtt{ND}}$ (d) $\mathcal{E}_N^{\mathtt{VD}}$

FIGURE 1. Variable Step DLN (12) with $Tol = 0.15, Re = 10,000, \theta = \frac{2}{3}, C_s = 0.1, \mu = 0.4$. We do not see backscatter in $\mathcal{E}_N^{\mathtt{MD}}$.

5.2. Test2. Flow between offset cylinder. We choose the 2D offset cylinder problem proposed by Jiang and Layton [33] to see whether the CSM (1) admits the transfer of energy from fluctuations back to means in the turbulent flow. Meanwhile, we would like to see how the time adaptive algorithm affects the occurrence of the

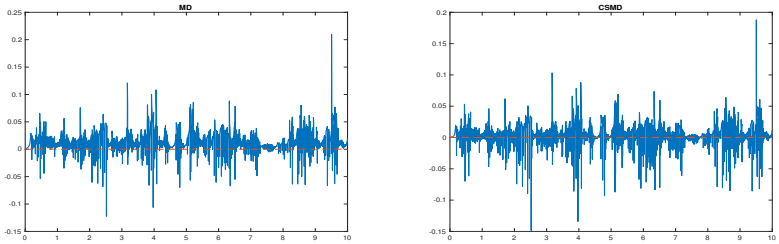

(a) $\mathcal{E}_N^{\texttt{MD}}$ (b) $\mathcal{E}_N^{\texttt{CSMD}}$

(c) $\mathcal{E}_N^{\texttt{ND}}$ (d) $\mathcal{E}_N^{\texttt{VD}}$

FIGURE 2. Variable Step DLN (12) with $Tol = 0.15, Re = 10,000, \theta = \frac{2}{\sqrt{5}}, C_s = 0.1, \mu = 0.4$. We see backscatter in $\mathcal{E}_N^{\texttt{MD}}$.

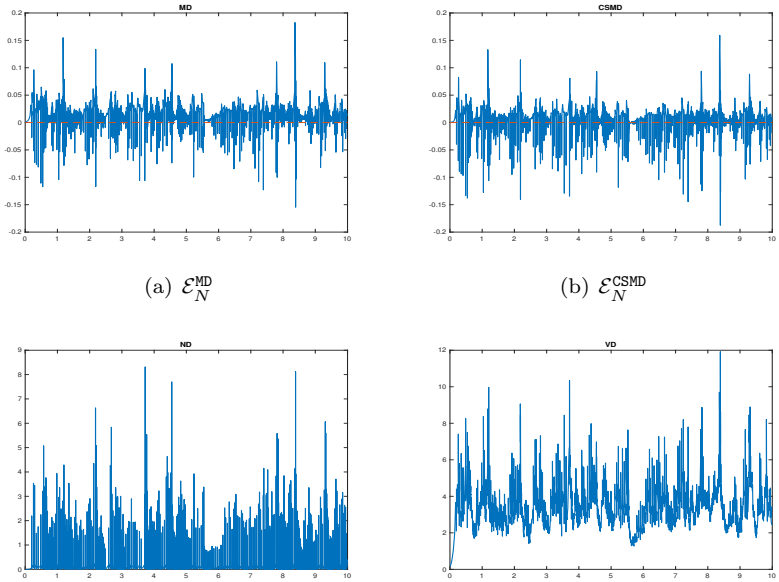

(a) $\mathcal{E}_N^{\texttt{MD}}$ (b) $\mathcal{E}_N^{\texttt{CSMD}}$

(c) $\mathcal{E}_N^{\texttt{ND}}$ (d) $\mathcal{E}_N^{\texttt{VD}}$

FIGURE 3. Variable Step DLN (12) with $Tol = 0.05, Re = 10,000, \theta = 0.95, C_s = 0.1, \mu = 0.4$. We see backscatter in $\mathcal{E}_N^{\texttt{MD}}$.

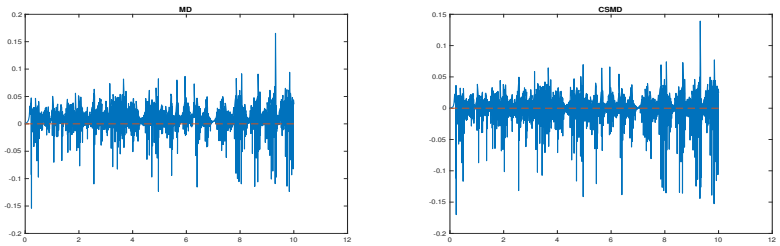

(a) $\mathcal{E}_N^{\mathtt{MD}}$ (b) $\mathcal{E}_N^{\mathtt{CSMD}}$

(c) $\mathcal{E}_N^{\mathtt{ND}}$ (d) $\mathcal{E}_N^{\mathtt{VD}}$

FIGURE 4. Variable Step DLN (12) with $Tol = 0.01, Re = 10,000, \theta = 0.98, C_s = 0.1, \mu = 0.4$. We see backscatter in $\mathcal{E}_N^{\mathtt{MD}}$.

backscatter phenomenon. The domain Ω is a unit disk centered at the origin with a smaller off-center obstacle inside, i.e. $\Omega = \{(x,y) : x^2+y^2 < 1,\ (x-0.5)^2+y^2 > 0.1^2\}$. The flow is driven by a counterclockwise rotational body force

$$f(x,y,t) = [-4y(1-x^2-y^2), 4x(1-x^2-y^2)]^{\mathrm{tr}},$$

with no-slip boundary conditions on both circles. Since the flow is driven by a counterclockwise force ($f = 0$ on the outer circle), it rotates about the origin and interacts with the immersed circle. We use 400 nodes on the outer circle and 100 nodes on the inner circle for mesh generation. We set final time $T = 10$ and model parameters $C_s = 0.1$, $\mu = 0.4$, Re $= 10^4$, δ to be the shortest edge of all triangles (≈ 0.01129). The backscatter phenomenon is measured by the model dissipation $\mathcal{E}_N^{\mathtt{MD}}$:

$$\mathcal{E}_N^{\mathtt{MD}} = \mathcal{E}_N^{\mathtt{CSMD}} + \int_\Omega (C_s\delta)^2 |\nabla \widetilde{w_{N-1,\beta}^h}||\nabla w_{N-1,\beta}^h|^2 dx,$$

$$\mathcal{E}_N^{\mathtt{CSMD}} = \int_\Omega \left(\frac{C_s^4\delta^2}{\mu^2} \frac{\alpha_2\nabla w_N^h + \alpha_1\nabla w_{N-1}^h + \alpha_0\nabla w_{N-2}^h}{\widehat{k}_{N-1}} \cdot \nabla w_{N-1,\beta}^h \right) dx.$$

Larger oscillations of $\mathcal{E}_N^{\mathtt{MD}}$ around zero means significant backscatter phenomenon. Thus only $\mathcal{E}_N^{\mathtt{CSMD}}$ makes contribution to backscatter. To design a time adaptive mechanism for the variable time-stepping DLN method, we adopt the minimum dissipation criteria proposed by F. Capuano, B. Sanderse, E. M. De Angelis, and G. Coppola [10]: time step k_n is adjusted to ensure the ratio of numerical dissipation

TABLE 3. Total time steps taken to reach $T = 10$ while using variable DLN for different values of θ.

θ	Tol	Total time steps	Backscatter observed
0.98	**0.01**	**9575**	Yes
0.95	0.01	6505	No
0.95	**0.05**	**1604**	Yes
$2/\sqrt{5}$	0.01	8988	No
$2/\sqrt{5}$	0.05	5680	No
$\mathbf{2/\sqrt{5}}$	**0.15**	**1973**	Yes
2/3	0.01	9944	No
2/3	0.05	9575	No
2/3	0.15	7149	No

$\mathcal{E}_{n+1}^{\mathtt{ND}}$ and viscous dissipation $\mathcal{E}_{n+1}^{\mathtt{VD}}$ is less than required tolerance `Tol`, i.e.

$$\chi_{n+1} = \frac{\mathcal{E}_{n+1}^{\mathtt{ND}}}{\mathcal{E}_{n+1}^{\mathtt{VD}}} < \mathtt{Tol}.$$

If the above criterion is satisfied, we accept the result of the current step and double the time step for the next step calculation. Otherwise, we halve the current time step for re-computing. We set the maximum time step $k_{\max} = 0.025$ for accuracy and minimum time step $k_{\min} = 0.0001$ for efficiency. The initial time step k_0 equals $k_{\min}$ and initial conditions are obtained by solving the steady Stokes problem with the same body force $f(x, y, t)$ and same Re. Tolerance `Tol` is pre-set each time to achieve the backscatter phenomenon to the largest possibility.

We first attempt the adaptive DLN algorithms with $\theta = 2/3$ and $\mathtt{Tol} = 0.15$. From Figure 1, we don't see the backscatter phenomenon since $\mathcal{E}_N^{\mathtt{CSMD}}$ is overwhelmed by second term in $\mathcal{E}_{n+1}^{\mathtt{ND}}$. Then we try the adaptive DLN algorithms with $\theta = 2/\sqrt{5}$ and same `Tol`. This time we observe evident backscatter in Figure 2. Hence, it's reasonable to expect that the backscatter phenomenon is more significant if θ is larger. Then we try the adaptive DLN algorithms with $\theta = 0.95$ and $\mathtt{Tol} = 0.05$. We observe more significant backscatter phenomenon in Figure 3. Lastly we increase θ to 0.98 and decrease `Tol` to 0.01 and still achieve large oscillations of $\mathcal{E}_{n+1}^{\mathtt{ND}}$ around zero in Figure 4. We also attempt these four θ values with different tolerance and summarize the results in Table 3. Table 3 shows that it's more likely to have backscatter phenomena by the adaptive DLN algorithms with larger θ. Also for relatively small θ values, we can increase `Tol` (larger average time step size) to have backscatter phenomena more easily.

Then we apply the constant time-stepping DLN algorithm in (11) with $k = 0.001$ to the same problem. From Figures 5 to 8, there is no backscatter phenomenon for all four θ values, which implies that it's more likely to have the backscatter phenomenon during the simulations with adaptive DLN algorithms. Moreover, we couldn't see the backscatter phenomenon unless we increase θ to 1 (See Figure 9). The oscillations in the model dissipation may come from the effect of normal ringing [5], which is seen in the standard midpoint rule.

Finally, we check how the new kinetic energy penalization in CSM affects the kinetic energy $\mathrm{KE} = \frac{1}{2}\|w_N^h\|^2$. We try different combinations of θ and `Tol` for adaptive DLN algorithms and observe that the KE stabilizes or only varies within a small range when backscatter happens. On the other hand, KE continues to increase with no backscatter phenomena. Figure 10 confirms our observation. The

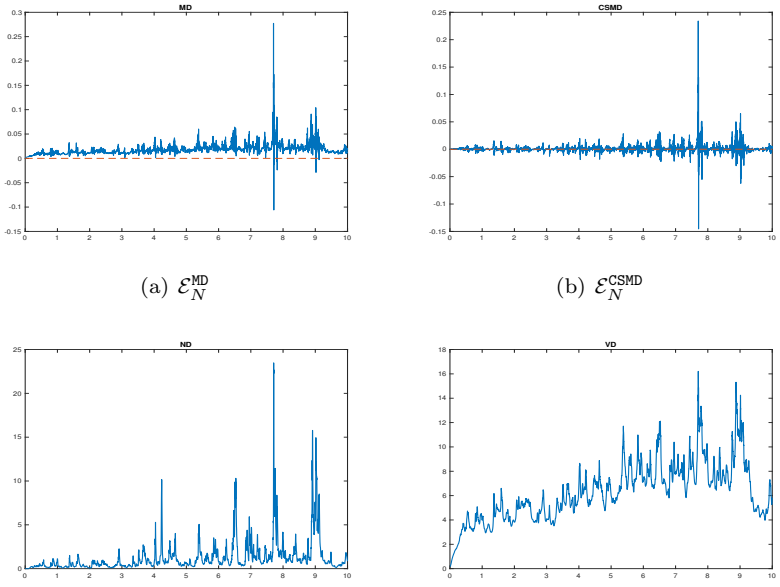

(a) $\mathcal{E}_N^{\mathtt{MD}}$ (b) $\mathcal{E}_N^{\mathtt{CSMD}}$

(c) $\mathcal{E}_N^{\mathtt{ND}}$ (d) $\mathcal{E}_N^{\mathtt{VD}}$

FIGURE 5. Constant time step DLN (12) with $k = 0.001, Re = 10,000, \theta = 0.98, C_s = 0.1, \mu = 0.4$. We do not see backscatter in $\mathcal{E}_N^{\mathtt{MD}}$.

left picture is the result of adaptive DLN algorithm with $\theta = 0.95$ and $\mathtt{Tol} = 0.01$. The kinetic energy continues to increase after a long time with no backscatter phenomenon happening (See Table 3). The right picture shows the converse: the adaptive DLN algorithm with $\theta = 0.95$ and $\mathtt{Tol} = 0.05$ has kinetic energy around 42 with significant backscatter phenomenon (See Table 3).

6. Conclusion

In the report, we propose the variable time-stepping DLN algorithm for the CSM and present a complete numerical analysis of the algorithm. In the stability analysis, we have shown that the numerical solutions are unconditionally stable in energy over the long term. In the error analysis, we have proved that the numerical velocity converges at second order under mild time step limits if the highest polynomial degrees satisfy $r = 2$ and $s = 1$, which is verified by the first numerical test problem in Subsection 5.1. It's clear that to get the backscattering phenomenon not from the ringing property of the method, we need dissipative methods and we need some control of numerical dissipation, $\mathcal{E}_N^{\mathtt{ND}}$. We therefore test in Subsection 5.2 by adapting the time step using minimum dissipation criteria. The closer $\theta = 1$, the closer the DLN method gets to be exactly conservative. If it is exactly conservative, we do not need tight control over $\mathcal{E}_N^{\mathtt{ND}}$. The further we go away from exactly conservative, the tighter control we need over $\mathcal{E}_N^{\mathtt{ND}}$ to see what seems to be true. In the future, error analysis for a semi-implicit DLN algorithm for CSM to avoid time restriction could be proven since it's an important open problem. Furthermore, in 3D, storage can be an issue and hence analysis of the reduced storage penalty method is also an interesting problem.

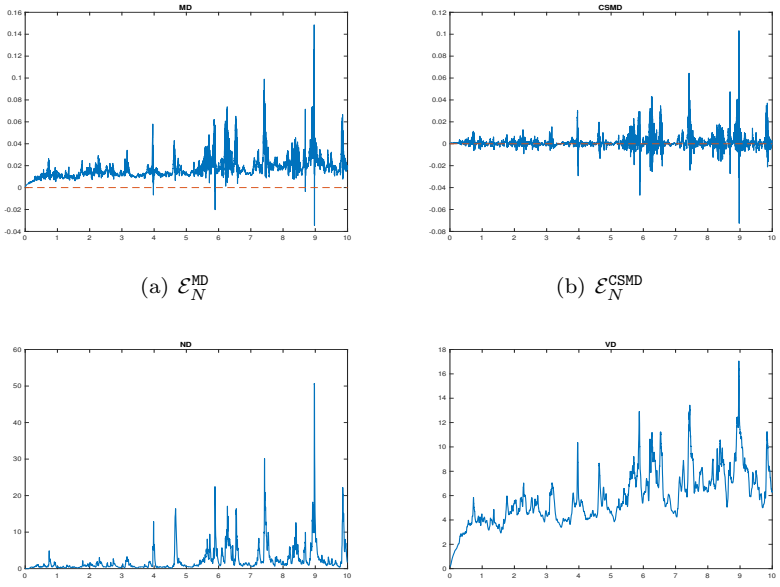

(a) $\mathcal{E}_N^{\texttt{MD}}$ (b) $\mathcal{E}_N^{\texttt{CSMD}}$

(c) $\mathcal{E}_N^{\texttt{ND}}$ (d) $\mathcal{E}_N^{\texttt{VD}}$

FIGURE 6. Constant time step DLN (12) with $k = 0.001, Re = 10,000, \theta = 0.95, C_s = 0.1, \mu = 0.4$. We do not see backscatter in $\mathcal{E}_N^{\texttt{MD}}$.

7. Appendix

In this appendix, we provide additional some additional tables and figures.

TABLE 4. Errors by $\|\cdot\|_{\infty,0}$-norm and Convergence Rate for the constant DLN with $\theta = 2/\sqrt{5}$.

k	h	$\|\|\|e^w\|\|\|_{\infty,0}$	Rate	$\|\|\|\nabla e^w\|\|\|_{\infty,0}$	Rate	$\|\|\|e^p\|\|\|_{\infty,0}$	Rate
0.08	0.08571	6.1375	-	59.5951	-	10.2725	-
0.04	0.04221	0.0499412	6.9412	1.35769	5.4560	0.0803944	6.9975
0.02	0.02095	0.0119888	2.0585	0.399817	1.7637	0.0195956	2.0366
0.01	0.01048	0.00297839	2.0091	0.103952	1.9434	0.00502445	1.9635

TABLE 5. Errors by $\|\cdot\|_{0,0}$-norm and Convergence Rate for the constant DLN with $\theta = 2/\sqrt{5}$.

k	h	$\|\|\|e^w\|\|\|_{0,0}$	Rate	$\|\|\|\nabla e^w\|\|\|_{0,0}$	Rate	$\|\|\|e^p\|\|\|_{0,0}$	Rate
0.08	0.08571	8.05856	-	86.5876	-	11.9822	-
0.04	0.04221	0.107272	6.2312	3.05843	4.8233	0.143556	6.3831
0.02	0.02095	0.0249452	2.1044	0.900625	1.7638	0.0346417	2.0510
0.01	0.01048	0.00616932	2.0156	0.234285	1.9427	0.00880143	1.9767

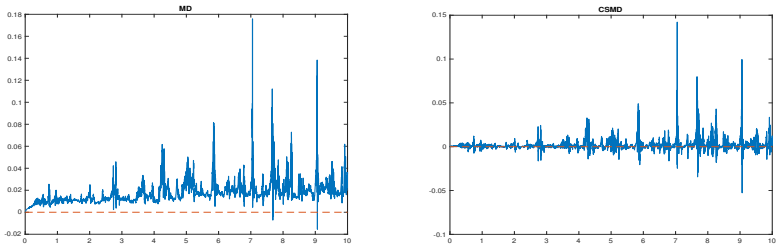

(a) $\mathcal{E}_N^{\mathtt{MD}}$ (b) $\mathcal{E}_N^{\mathtt{CSMD}}$

(c) $\mathcal{E}_N^{\mathtt{ND}}$ (d) $\mathcal{E}_N^{\mathtt{VD}}$

FIGURE 7. Constant time step DLN (12) with $k = 0.001, Re = 10,000, \theta = \frac{2}{\sqrt{5}}, C_s = 0.1, \mu = 0.4$. We do not see backscatter in $\mathcal{E}_N^{\mathtt{MD}}$.

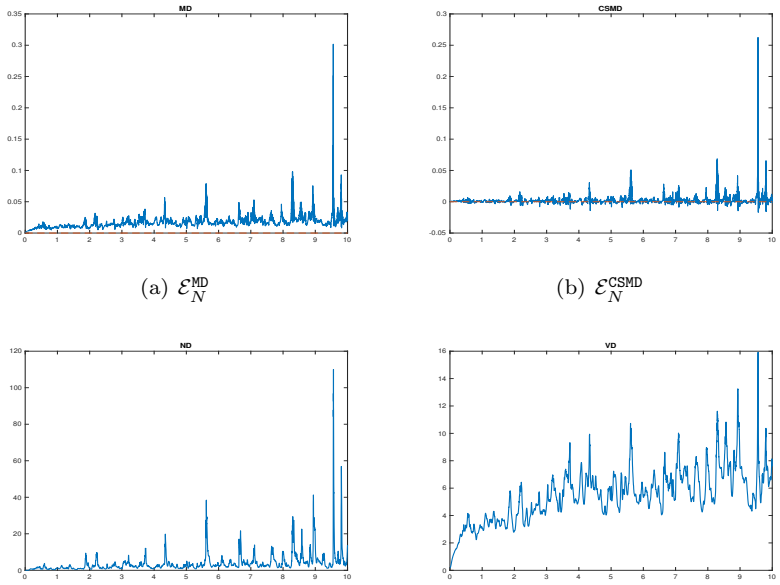

(a) $\mathcal{E}_N^{\mathtt{MD}}$ (b) $\mathcal{E}_N^{\mathtt{CSMD}}$

(c) $\mathcal{E}_N^{\mathtt{ND}}$ (d) $\mathcal{E}_N^{\mathtt{VD}}$

FIGURE 8. Constant time step DLN (12) with $k = 0.001, Re = 10,000, \theta = \frac{2}{3}, C_s = 0.1, \mu = 0.4$. We do not see backscatter in $\mathcal{E}_N^{\mathtt{MD}}$.

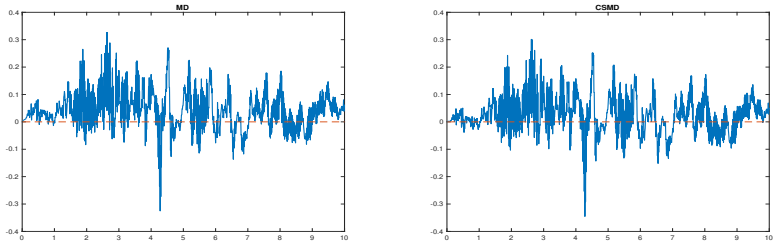

(a) $\mathcal{E}_N^{\mathtt{MD}}$ (b) $\mathcal{E}_N^{\mathtt{CSMD}}$

(c) $\mathcal{E}_N^{\mathtt{ND}}$ (d) $\mathcal{E}_N^{\mathtt{VD}}$

FIGURE 9. Constant time step DLN (12) with $k = 0.001, Re = 10,000, \theta = 1, C_s = 0.1, \mu = 0.4$.

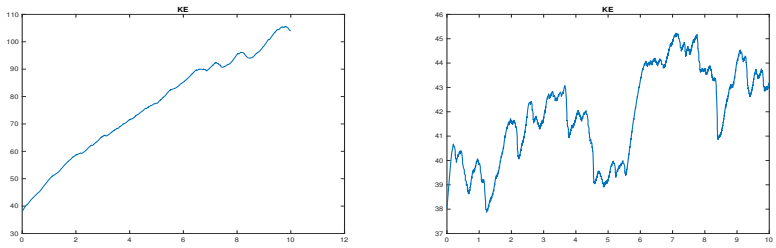

(a) KE, Tol=0.01 (b) KE, Tol=0.05

FIGURE 10. Variable Step DLN (12) with $Re = 10,000, \theta = 0.95, C_s = 0.1, \mu = 0.4$. The left picture is for no backscatter and the right picture is for backscatter.

TABLE 6. Errors by $\|\cdot\|_{\infty,0}$-norm and Convergence Rate for the constant DLN with $\theta = 1$.

k	h	$\|\|\|e^w\|\|\|_{\infty,0}$	Rate	$\|\|\|\nabla e^w\|\|\|_{\infty,0}$	Rate	$\|\|\|e^p\|\|\|_{\infty,0}$	Rate
0.08	0.08571	6.03148	-	72.2845	-	14.0717	-
0.04	0.04221	0.0499902	6.9147	1.35784	5.7343	0.0831369	7.4031
0.02	0.02095	0.0120016	2.0584	0.399858	1.7638	0.0203057	2.0336
0.01	0.01048	0.00298191	2.0089	0.103961	1.9434	0.00512713	1.9857

TABLE 7. Errors by $\|\cdot\|_{0,0}$-norm and Convergence Rate for the constant DLN with $\theta = 1$.

k	h	$\|\|\|e^w\|\|\|_{0,0}$	Rate	$\|\|\|\nabla e^w\|\|\|_{0,0}$	Rate	$\|\|\|e^p\|\|\|_{0,0}$	Rate
0.08	0.08571	8.50684	-	105.23	-	14.0354	-
0.04	0.04221	0.107277	6.3092	3.05802	5.1048	0.14397	6.6072
0.02	0.02095	0.0249479	2.1044	0.90061	1.7636	0.0347625	2.0502
0.01	0.01048	0.0061698	2.0156	0.234279	1.9427	0.00883384	1.9764

Acknowledgments

We would like to thank Dr. W. J. Layton, for his insightful idea and guidance throughout the research. This research is partially supported by the NSF grant DMS-2110379.

References

[1] C. Amrouche and L. C. Berselli and R. Lewandowski and D. D. Nguyen. Turbulent flows as generalized Kelvin–Voigt materials: Modeling and analysis. Nonlinear Analysis, Elsevier, 196:111790, 2020.

[2] U. M. Ascher and L. R. Petzold. Computer methods for ordinary differential equations and differential-algebraic equations. Society for Industrial and Applied Mathematics (SIAM), Philadelphia, PA, 1998.

[3] E. S. Baranovskii. Strong solutions of the incompressible Navier–Stokes–Voigt model. Mathematics, 8(2):181,2020.

[4] J. Bardina, J. Ferziger, and W. C. Reynolds. Improved subgrid-scale models for large-eddy simulation. In 13th fluid and plasmadynamics conference, page 1357, 1980.

[5] J. Burkardt, W. Pei, and C. Trenchea. A stress test for the midpoint time-stepping method. Int. J. Numer. Anal. Model., 19(2-3):299–314, 2022.

[6] S. C. Brenner and L. R. Scott. The mathematical theory of finite element methods, volume 15 of Texts in Applied Mathematics. Springer, New York, third edition, 2008.

[7] M. Bukač, A. Seboldt, and C. Trenchea. Refactorization of Cauchy's method: a second-order partitioned method for fluid-thick structure interaction problems. J. Math. Fluid Mech., 23(3):Paper No. 64, 25, 2021.

[8] J. Burkardt and C. Trenchea. Refactorization of the midpoint rule. Appl. Math. Lett., 107:106438, 7, 2020.

[9] M. Bukač and C. Trenchea. Adaptive, second-order, unconditionally stable partitioned method for fluid-structure interaction. Comput. Methods Appl. Mech. Engrg., 393:Paper No. 114847, 24, 2022.

[10] F. Capuano, B. Sanderse, E. M. D. Angelis, and G. Coppola. A minimum-dissipation time-integration strategy for large-eddy simulation of incompressible turbulent flows. AIMETA 2017 Proceedings of the XXIII Conference of the Italian Association of Theoretical and Applied Mechanics, pages 2311–2323, 2017.

[11] M. A. Case, V. J. Ervin, A. Linke, and L. G. Rebholz. A connection between Scott-Vogelius and grad-div stabilized Taylor-Hood FE approximations of the Navier-Stokes equations. SIAM J. Numer. Anal., 49(4):1461–1481, 2011.

[12] N. Chorfi, M. Abdelwahed, and L. C. Berselli. On the analysis of a geometrically selective turbulence model. Adv. Nonlinear Anal., 9(1):1402–1419, 2020.

[13] P. G. Ciarlet. The finite element method for elliptic problems. Studies in Mathematics and its Applications, Vol. 4. North-Holland Publishing Co., Amsterdam-New York-Oxford, 1978.

[14] G. G. Dahlquist. On the relation of G-stability to other stability concepts for linear multistep methods. Dept. of Comp. Sci. Roy. Inst. of Technology, Report TRITA-NA-7621, 1976.

[15] G. G. Dahlquist. *G*-stability is equivalent to *A*-stability. BIT, 18(4):384–401, 1978.

[16] G. G. Dahlquist. Positive functions and some applications to stability questions for numerical methods. In Recent advances in numerical analysis (Proc. Sympos., Math. Res. Center, Univ. Wisconsin, Madison, Wis., 1978), volume 41 of Publ. Math. Res. Center Univ. Wisconsin, pages 1–29. Academic Press, New York-London, 1978.

[17] Q. Du and M. D. Gunzburger. Analysis of a Ladyzhenskaya model for incompressible viscous flow. J. Math. Anal. Appl., 155(1):21–45, 1991.

[18] T. Dai, S. Liu, J. Liu, N. Jiang, and Q. Chen. Development of a new dynamic Smagorinsky model by an artificial neural network for prediction of outdoor airflow and pollutant dispersion. Building and Environment, page 110624, 2023.
[19] G. G. Dahlquist, W. Liniger, and O. Nevanlinna. Stability of two-step methods for variable integration steps. SIAM J. Numer. Anal., 20(5):1071–1085, 1983.
[20] P. A. Durbin and B. A. Pettersson Reif. Statistical theory and modeling for turbulent flows. John Wiley & Sons, Ltd., Chichester, second edition, 2011.
[21] J. H. Ferziger and M. Perić. Computational methods for fluid dynamics. Springer-Verlag, Berlin, revised edition, 1999.
[22] G.P. Galdi and W.J. Layton. Approximation of the larger eddies in fluid motions. II. A model for space-filtered flow. Math. Models Methods Appl. Sci., 10(3):343–350, 2000.
[23] J. L. Guermond, P. Minev, and J. Shen. An overview of projection methods for incompressible flows. Comput. Methods Appl. Mech. Engrg., 195(44-47):6011–6045, 2006.
[24] V. Girault and P. A. Raviart. Finite element approximation of the Navier-Stokes equations, volume 749 of Lecture Notes in Mathematics. Springer-Verlag, Berlin, 1979.
[25] V. Girault and P. Raviart. Finite element methods for Navier-Stokes equations, volume 5 of Springer Series in Computational Mathematics. Springer-Verlag, Berlin, 1986. Theory and algorithms.
[26] E. Hairer, S. P. Nørsett, and G. Wanner. Solving ordinary differential equations. I, volume 8 of Springer Series in Computational Mathematics. Springer-Verlag, Berlin, second edition, 1993. Nonstiff problems.
[27] J. G. Heywood and R. Rannacher. Finite-element approximation of the nonstationary Navier-Stokes problem. Part IV: Error analysis for second-order time discretization. SIAM Journal on Numerical Analysis, 27(2):353–384, 1990.
[28] T. Iliescu, V. John, W. J. Layton, G. Matthies, and L. Tobiska. A numerical study of a class of LES models. Int. J. Comput. Fluid Dyn., 17(1):75–85, 2003.
[29] T. Iliescu and W. J. Layton. Approximating the larger eddies in fluid motion. III. The Boussinesq model for turbulent fluctuations. An. Ştiinţ. Univ. Al. I. Cuza Iaşi. Mat. (N.S.), 44(2):245–261 (2000), 1998.
[30] R. Ingram. A new linearly extrapolated crank-nicolson time-stepping scheme for the Navier-Stokes equations. Mathematics of Computation, 82(284):1953–1973, 2013.
[31] R. Ingram. Unconditional convergence of high-order extrapolations of the Crank-Nicolson, finite element method for the Navier-Stokes equations. Int. J. Numer. Anal. Model., 10(2):257–297, 2013.
[32] N. Jiang and W. Layton. An algorithm for fast calculation of flow ensembles. Int. J. Uncertain. Quantif., 4(4):273–301, 2014.
[33] N. Jiang and W. Layton. Algorithms and models for turbulence not at statistical equilibrium. Comput. Math. Appl., 71(11):2352–2372, 2016.
[34] N. Jiang and W. J. Layton and M. McLaughlin and Y. Rong and H. Zhao. On the Foundations of Eddy Viscosity Models of Turbulence. Fluids, 5(4):99–137, 2020.
[35] V. John. Finite element methods for incompressible flow problems, volume 51 of Springer Series in Computational Mathematics. Springer, Cham, 2016.
[36] V. John and W. J. Layton. Analysis of numerical errors in large eddy simulation. SIAM J. Numer. Anal., 40(3):995–1020, 2002.
[37] T. K. Kim. A modified Smagorinsky subgrid scale model for the large eddy simulation of turbulent flow. University of California, Davis, 2001.
[38] A. N. Kolmogorov. Equations of turbulent motion of an incompressible fluid, Izv. Acad. Sci., USSR. Physics, 6(1):2, 1942.
[39] P. Kuberry, A. Larios, L. G. Rebholz, and N. E. Wilson. Numerical approximation of the Voigt regularization for incompressible Navier-Stokes and magnetohydrodynamic flows. Comput. Math. Appl., 64(8):2647–2662, 2012.
[40] G. Y. Kulikov and S. K. Shindin. On stable integration of stiff ordinary differential equations with global error control. In International Conference on Computational Science (1), pages 42–49, 2005.
[41] G. Y. Kulikov and S. K. Shindin. One-leg integration of ordinary differential equations with global error control. Computational Methods in Applied Mathematics, 5(1):86–96, 2005.
[42] D. K. Lilly. The representation of small-scale turbulence in numerical simulation experiments, H. H. Goldstine, Ed., Proceedings of IBM Scientific Computing Symposium on Environmental Sciences, Yorktown Heights, New York, pp. 195-210, 1967.

[43] A. Labovsky, W. J. Layton, C. C. Manica, M. Neda, and L. G. Rebholz. The stabilized extrapolated trapezoidal finite-element method for the Navier-Stokes equations. Comput. Methods Appl. Mech. Engrg., 198(9-12):958–974, 2009.
[44] W. J. Layton. A nonlinear, subgridscale model for incompressible viscous flow problems. SIAM J. Sci. Comput., 17(2):347–357, 1996.
[45] W. Layton and M. McLaughlin. Doubly-adaptive artificial compression methods for incompressible flow. J. Numer. Math., 28(3):179–196, 2020.
[46] W. Layton, W. Pei, Y. Qin, and C. Trenchea. Analysis of the variable step method of Dahlquist, Liniger and Nevanlinna for fluid flow. Numer. Methods Partial Differential Equations, 38(6):1713–1737, 2022.
[47] W. Layton, W. Pei, and C. Trenchea. Refactorization of a variable step, unconditionally stable method of Dahlquist, Liniger and Nevanlinna. Appl. Math. Lett., 125:Paper No. 107789, 7, 2022.
[48] W. Layton, W. Pei, and C. Trenchea. Time step adaptivity in the method of Dahlquist, Liniger and Nevanlinna. Advances in Computational Science and Engineering, 1(3):320–350, 2023.
[49] A. Larios, M. R. Petersen, E. S. Titi, and B. Wingate. A computational investigation of the finite-time blow-up of the 3D incompressible Euler equations based on the Voigt regularization. Theor. Comput. Fluid Dyn., 32(1):23–34, 2018.
[50] A. Larios and E. S. Titi. Higher-order global regularity of an inviscid Voigt-regularization of the three-dimensional inviscid resistive magnetohydrodynamic equations. J. Math. Fluid Mech., 16(1):59–76, 2014.
[51] J. Mathieu and J. Scott. An introduction to turbulent flow. Cambridge University Press, Cambridge, 2000.
[52] A. Pakzad. Damping functions correct over-dissipation of the Smagorinsky model. Math. Methods Appl. Sci., 40(16):5933–5945, 2017.
[53] W. Pei. The Semi-implicit DLN Algorithm for the Navier Stokes Equations. Numerical Algorithms, 2024.
[54] L. Prandtl. Über ein neues Formelsystem für die ausgebildete Turbulenz. Nachrichten der Akademie der Wissenschaften zu Göttingen, Mathematisch-Physikalische Klasse. Vandenhoeck & Ruprecht, 1945.
[55] Y. Qin, L. Chen, Y. Wang, Y. Li, and J. Li. An adaptive time-stepping DLN decoupled algorithm for the coupled Stokes-Darcy model. Appl. Numer. Math., 188:106–128, 2023.
[56] Y. Qin, Y. Hou, W. Pei, and J. Li. A variable time-stepping algorithm for the unsteady Stokes/Darcy model. J. Comput. Appl. Math., 394:Paper No. 113521, 14, 2021.
[57] Y. Rong, W. Layton, and H. Zhao. Extension of a simplified Baldwin-Lomax model to nonequilibrium turbulence: model, analysis and algorithms. Numer. Methods Partial Differential Equations, 35(5):1821–1846, 2019.
[58] R. S. Rogallo and P. Moin. Numerical simulation of turbulent flows. Annual Review of Fluid Mechanics, 16(1):99–137, 1984.
[59] F. Siddiqua and X. Xie. Numerical analysis of a corrected Smagorinsky model. Numer. Methods Partial Differential Equations, 39(1):356–382, 2023.
[60] J. Smagorinsky. General circulation experiments with the primitive equations. Monthly Weather Review, 91(3):99–164, 1963.

Department of Mathematics, University of Pittsburgh, Pittsburgh, PA 15260, USA
E-mail: fas41@pitt.edu
URL: https://sites.pitt.edu/~fas41/

Department of Mathematics, The Ohio State University, Columbus, OH 43210, USA
E-mail: pei.176@osu.edu
URL: https://math.osu.edu/people/pei.176